

*Atmospheric Measurement Techniques Discussions* is the access reviewed discussion forum of *Atmospheric Measurement Techniques*

**An analysis of  
precision  
requirements and  
flux errors**

V. Wolff et al.

# **Aerodynamic gradient measurements of the $\text{NH}_3\text{-HNO}_3\text{-NH}_4\text{NO}_3$ triad using a wet chemical instrument: an analysis of precision requirements and flux errors**

**V. Wolff<sup>1</sup>, I. Trebs<sup>1</sup>, C. Ammann<sup>2</sup>, and F. X. Meixner<sup>1,3</sup>**

<sup>1</sup>Max Planck Institute for Chemistry, Biogeochemistry and Air Chemistry Department, P.O. Box 3060, 55020 Mainz, Germany

<sup>2</sup>Agroscope ART, Air Pollution and Climate Group, 8046 Zürich, Switzerland

<sup>3</sup>Department of Physics, University of Zimbabwe, P.O. Box MP 167, Harare, Zimbabwe

Received: 15 July 2009 – Accepted: 21 September 2009 – Published: 8 October 2009

Correspondence to: V. Wolff (veronika.wolff@mpic.de)

Published by Copernicus Publications on behalf of the European Geosciences Union.

Title Page

Abstract

Introduction

Conclusions

References

Tables

Figures

⏪

⏩

◀

▶

Back

Close

Full Screen / Esc

Printer-friendly Version

Interactive Discussion

## Abstract

The aerodynamic gradient method is widely used for flux measurements of ammonia, nitric acid, particulate ammonium nitrate (the  $\text{NH}_3$ - $\text{HNO}_3$ - $\text{NH}_4\text{NO}_3$  triad) and other water-soluble reactive trace compounds. The surface exchange flux is derived from a measured concentration difference and micrometeorological quantities (turbulent exchange coefficient). The significance of the measured concentration difference is crucial for the significant determination of surface exchange fluxes. Additionally, measurements of surface exchange fluxes of ammonia, nitric acid and ammonium nitrate are often strongly affected by phase changes between gaseous and particulate compounds of the triad, which make measurements of the four individual species ( $\text{NH}_3$ ,  $\text{HNO}_3$ ,  $\text{NH}_4^+$ ,  $\text{NO}_3^-$ ) necessary for a correct interpretation of the measured concentration differences.

We present here a rigorous analysis of results obtained with a multi-component, wet-chemical instrument, able to simultaneously measure gradients of both gaseous and particulate trace substances. Basis for our analysis are two field experiments, conducted above contrasting ecosystems (grassland, forest). Precision requirements of the instrument as well as errors of concentration differences and micrometeorological exchange parameters have been estimated, which, in turn, allows the establishment of thorough error estimates of the derived fluxes of  $\text{NH}_3$ ,  $\text{HNO}_3$ ,  $\text{NH}_4^+$ , and  $\text{NO}_3^-$ . Derived median flux errors for the grassland and forest field experiments were: 39 and 50% ( $\text{NH}_3$ ), 31 and 38% ( $\text{HNO}_3$ ), 62 and 57% ( $\text{NH}_4^+$ ), and 47 and 68% ( $\text{NO}_3^-$ ), respectively. Additionally, we provide the basis for using field data to characterize the instrument performance, as well as subsequent quantification of surface exchange fluxes and underlying mechanistic processes under realistic ambient measurement conditions.

## An analysis of precision requirements and flux errors

V. Wolff et al.

Title Page

Abstract

Introduction

Conclusions

References

Tables

Figures

⏪

⏩

◀

▶

Back

Close

Full Screen / Esc

Printer-friendly Version

Interactive Discussion

## 1 Introduction

Ammonia ( $\text{NH}_3$ ) is the most abundant alkaline gas in the atmospheric boundary layer. It is important for neutralising acids and strongly influences the chemical composition of particles (Seinfeld and Pandis, 2006). Major sources of  $\text{NH}_3$  are agricultural and other anthropogenic activities (Sutton et al., 2000a). Gaseous nitric acid ( $\text{HNO}_3$ ) is the major sink of nitrogen oxides, emitted primarily through combustion of fossil fuels.  $\text{HNO}_3$  is removed from the atmosphere by dry and wet deposition leading, at least in part, to the formation of “acid rain” (Seinfeld and Pandis, 2006; Calvert et al., 1985) and, therefore, has an immediate impact on the biosphere. Gaseous  $\text{NH}_3$  and  $\text{HNO}_3$  can react in the atmosphere to form solid or dissolved ammonium nitrate ( $\text{NH}_4\text{NO}_3$ ).  $\text{NH}_3$ ,  $\text{HNO}_3$  and  $\text{NH}_4\text{NO}_3$  usually establish a reversible thermodynamic phase equilibrium which is dependent on relative humidity and temperature (e.g., Mozurkewich, 1993; Stelson and Seinfeld, 1982).  $\text{NH}_4\text{NO}_3$  is therefore semi-volatile under typical atmospheric conditions. Increasing emissions of  $\text{NH}_3$  and precursor gases of  $\text{HNO}_3$  (Galloway et al., 2004) and subsequent enhanced  $\text{NH}_3$  and  $\text{HNO}_3$  deposition, have substantial environmental impacts, such as eutrophication (Remke et al., 2009), acidification (Erisman et al., 2008), loss of biodiversity in ecosystems (Kleijn et al., 2009; Krupa, 2003). They may also cause human health problems due to increased particle formation (Erisman and Schaap, 2004). In order to address these problems, so-called critical loads have been introduced, as quantitative estimates of the deposition of one or more pollutants below which significant harmful effects on specified elements of the environment do not occur according to the present knowledge (Cape et al., 2009; Plassmann et al., 2009). Hence, the knowledge of exchange processes and deposition rates of these compounds is fundamental for atmospheric research and for policy makers.

$\text{NH}_3$  and  $\text{HNO}_3$  are polar molecules, which are highly water-soluble and exhibit a high affinity towards surfaces. Therefore, the measurement of these compounds with high temporal resolution is a challenge under atmospheric conditions. Particulate compounds usually feature low deposition velocities, hence they typically exhibit very

## An analysis of precision requirements and flux errors

V. Wolff et al.

Title Page

Abstract

Introduction

Conclusions

References

Tables

Figures

⏪

⏩

◀

▶

Back

Close

Full Screen / Esc

Printer-friendly Version

Interactive Discussion

---

**An analysis of  
precision  
requirements and  
flux errors**V. Wolff et al.

---

[Title Page](#)[Abstract](#)[Introduction](#)[Conclusions](#)[References](#)[Tables](#)[Figures](#)[⏪](#)[⏩](#)[◀](#)[▶](#)[Back](#)[Close](#)[Full Screen / Esc](#)[Printer-friendly Version](#)[Interactive Discussion](#)

small concentration gradients in the surface layer, demanding high precision instruments to measure vertical concentration differences of these species (e.g., Erisman et al., 1997). To characterize the surface exchange of the  $\text{NH}_3$ - $\text{HNO}_3$ - $\text{NH}_4\text{NO}_3$  triad, simultaneous measurements of  $\text{NH}_3$ ,  $\text{HNO}_3$ , particulate  $\text{NH}_4^+$  and  $\text{NO}_3^-$  are mandatory and they should be highly selective with respect to gaseous and particulate phases.

Direct measurements of surface-atmosphere exchange fluxes may be provided by the eddy covariance method, but it requires fast response trace gas sensors. Some newly developed fast instruments have been tested and validated recently (e.g., Schmidt and Klemm, 2008; Farmer et al., 2006; Zheng et al., 2008; Brodeur et al., 2009; Huey, 2007; Nemitz et al., 2008). Their major drawback is the restricted applicability to a single compound, not allowing for the characterization of the entire  $\text{NH}_3$ - $\text{HNO}_3$ - $\text{NH}_4\text{NO}_3$  triad. Moreover these instruments are still under development, and their detection limit is still too high to measure in remote environments (Nemitz et al., 2000).

Thus, to date, the aerodynamic gradient method (AGM) is still the commonly applied technique to measure  $\text{NH}_3$ ,  $\text{HNO}_3$  and  $\text{NH}_4\text{NO}_3$  surface exchange fluxes (e.g., Businger, 1986; Erisman and Wyers, 1993; Phillips et al., 2004; Nemitz et al., 2004a). Surface-atmosphere exchange fluxes are derived from measurements of vertical concentration differences by instruments with much lower time resolution than covariance techniques. The AGM requires average concentrations (over 30–60 min) measured at two or more heights above the investigated surface or vegetation canopy.

Most studies that investigated the surface-atmosphere exchange fluxes of  $\text{NH}_3$ ,  $\text{HNO}_3$  and particulate  $\text{NH}_4^+$  and  $\text{NO}_3^-$  did not consider errors of the applied measurement techniques, nor did they present errors of the calculated fluxes and deposition velocities (Businger and Delany, 1990). However, error estimates and/or confidence intervals of the results are an important part of a thorough analysis and presentation of any measurement results and their scientific interpretation (Miller and Miller, 1988).

In this study, we evaluate the performance of the novel GRAEGOR instrument (GRAdient of AErosol and Gases Online Registrar; ECN, Petten, NL) recently described

---

**An analysis of  
precision  
requirements and  
flux errors**V. Wolff et al.

---

[Title Page](#)[Abstract](#)[Introduction](#)[Conclusions](#)[References](#)[Tables](#)[Figures](#)[◀](#)[▶](#)[◀](#)[▶](#)[Back](#)[Close](#)[Full Screen / Esc](#)[Printer-friendly Version](#)[Interactive Discussion](#)

by Thomas et al. (2009) for aerodynamic gradient measurements of  $\text{NH}_3$ ,  $\text{HNO}_3$ ,  $\text{NH}_4^+$ , and  $\text{NO}_3^-$  to determine exchange fluxes under representative environmental conditions. GRAEGOR is a wet chemical instrument for the quasi-continuous measurement of two-point vertical concentration differences of water-soluble reactive trace gas species and their related particulate compounds. We use results from two field campaigns to investigate (a) the precision requirements of the concentration measurements above different ecosystems under varying micrometeorological conditions, (b) the error of the concentration difference measured with GRAEGOR, (c) the error of the micrometeorological exchange parameter (the transfer velocity,  $v_{tr}$ ), and (d) the resulting flux error. The experiments were conducted over contrasting ecosystems, a grassland site with low canopy height, low aerodynamic roughness and high nutrient input, and a spruce forest site with tall vegetation, high aerodynamic roughness and low nutrient state. Due to the differences in micrometeorological as well as in nutrient balance conditions, exchange processes are expected to be different.

For the first time, a wet-chemical multi-component instrument is characterized in terms of the instrument precision to resolve vertical concentration differences and the associated errors of surface-atmosphere exchange fluxes.

## 2 Experimental

### 2.1 Site descriptions

#### 2.1.1 Grassland site, Switzerland (NitroEurope)

Measurements were performed at an intensively managed grassland site in central Switzerland, close to the village of Oensingen ( $47^\circ 17' \text{ N}$ ,  $07^\circ 44' \text{ E}$ , 450 m a.s.l.) in summer 2006 (20 July–4 September) within the framework of the EU project “NitroEurope-IP” (Sutton et al., 2007). Intensive agriculture (grassland and arable crops) dominate the surrounding area. The climate is temperate continental, with a mean annual air

temperature of 9°C and an average rainfall of 1100 mm. The site, established in 2001, consists of two neighbouring 50×150 m<sup>2</sup> plots, one of them being fertilized (150–200 kg nitrate ha<sup>-1</sup> a<sup>-1</sup> in form of ammonium nitrate and slurry) and cut 4–5 times per year, the other one is not fertilized and is cut 2–3 times per year (Ammann et al., 2007).

The site has been used for studies of a variety of research areas, such as carbon and greenhouse gas budgets (Ammann et al., 2007; Flechard et al., 2005), ozone studies (Jaeggi et al., 2006) and nitrogen related studies (Neftel et al., 2007; Ammann et al., 2007; Norman et al., 2009). During the measurement period in 2006, temperatures were quite high in the beginning with maximum daytime temperatures of up to 35°C, night time temperatures of around 17°C, and relative humidities below 30%. This warm period was followed by some episodes of rain and cloud cover leading to lower temperatures (<10°C). The grassland consists of grass species as well as legumes and some herb species (Ammann et al., 2007), its canopy height grew during our study from around 0.08 to 0.25 m.

### 2.1.2 Spruce forest site, Germany (EGER)

The second experiment was conducted within the framework of the project EGER (ExchanGe processes in mountainous Regions) at the research site “Weidenbrunnen” (50°08' N, 11°52' E; 774 m a.s.l.), a Norway spruce forest site located in a mountainous region in south east Germany (Fichtelgebirge) in summer/autumn 2007 (25 August–3 October). The surrounding mountainous area extends approx. 1000 km<sup>2</sup> and is covered mainly with forest, agricultural land including meadows and lakes. It is located in the transition zone from maritime to continental climates with annual average temperatures of 5.0°C (1971–2000; Foken, 2003) and average annual precipitation sum of 1162 mm (1971–2000; Foken, 2003). The study site has been maintained for more than 10 years by the University of Bayreuth and a variety of studies have been conducted there (Held and Klemm, 2006; Klemm et al., 2006; Falge et al., 2005; Thomas and Foken, 2007; Rebmann et al., 2005; Wichura et al., 2004). The stand age of the Norway spruce (*Picea abies*) was approx. 54 years (according to Alsheimer, 1997),

## An analysis of precision requirements and flux errors

V. Wolff et al.

Title Page

Abstract

Introduction

Conclusions

References

Tables

Figures

⏪

⏩

◀

▶

Back

Close

Full Screen / Esc

Printer-friendly Version

Interactive Discussion



the mean canopy height was estimated to be 23 m (Staudt, 2007), and the single sided leaf area index was 5.3. Measurements were performed on a 31 m walk-up tower. During the EGER measurements in 2007, temperatures were generally quite low (around 10°C) and the relative humidity often remained above 80% throughout the day. Only a few days with higher temperatures of up to 22°C and lower relative humidity (50–60%) were encountered.

### 2.1.3 Measurement method

The GRAEGOR (Thomas et al., 2009) is a wet chemical instrument for semi-continuous, simultaneous two-point concentration measurements of water-soluble reactive trace gases (NH<sub>3</sub>, HNO<sub>3</sub>, HONO, HCl, and SO<sub>2</sub>) and their related particulate compounds (NH<sub>4</sub><sup>+</sup>, NO<sub>3</sub><sup>-</sup>, Cl<sup>-</sup>, SO<sub>4</sub><sup>2-</sup>). GRAEGOR collects the gas and particulate samples simultaneously at two heights using horizontally aligned wet-annular rotating denuders and steam-jet aerosol collectors (SJAC), respectively (see to Fig. 1). Air is simultaneously drawn through the sample boxes, passing first the wet-annular rotating denuders, where water-soluble gases diffuse from a laminar air stream into the sample liquid. In both SJACs, the sample air is then mixed with water vapour from double-deionized water and the supersaturation causes particles to grow rapidly (within 0.1 s) into droplets of at least 2 µm diameter. These droplets, containing the dissolved particulate species are then collected in a cyclone (cf. Trebs et al., 2004). The airflow through the two sample boxes is ~14 L min<sup>-1</sup> (at STP=0°C and 1013.25 hPa) per box and is kept constant by a critical orifice downstream of the SJAC. Liquid samples are sequentially analyzed online using ion chromatography (IC) for anions and flow injection analysis (FIA) for NH<sub>3</sub> and particulate NH<sub>4</sub><sup>+</sup>. Within each full hour GRAEGOR provides one half-hourly integrated gas and particulate concentration for each height for each species (one sequential analytical cycle of all four liquid samples (two denuder, two SJAC samples) takes 1 h, cf. Thomas et al., 2009).

Syringe pumps in the analytical box (Fig. 1) provide stable liquid flows, which has improved the accuracy of the instrument in comparison to previous studies (cf. Trebs

## An analysis of precision requirements and flux errors

V. Wolff et al.

Title Page

Abstract

Introduction

Conclusions

References

Tables

Figures

◀

▶

◀

▶

Back

Close

Full Screen / Esc

Printer-friendly Version

Interactive Discussion



et al., 2004). Prior to analysis an internal bromide standard is added to each sample. Additionally to its use in the determination of the concentration value, it is used in combination with monitoring the FIA waste flow as an internal quality indicator, enabling the identification of poor chromatograms (high/noisy baseline, bad peak shapes), high double-de-ionized water conductivity and unstable flows.

During NitroEurope (NEU) the inlets of the sample boxes, directly connected to the wet-annular rotating denuders, consisted of PFA (perfluoroalkoxy) Teflon tubing (I.D.=0.8 cm, length=30 cm), ending upstream in a PE-funnel covered by a mosquito net. NEU measurements were made in the middle of an intensively managed plot, and, according to the available fetch (Ammann et al., 2007; Neftel et al., 2008), measurement heights were chosen to be 1.23 and 0.37 m above ground. During EGER, measurements were performed on a walk-up tower and the sample boxes were located on 24.4 and 30.9 m above ground. The PFA Teflon tubing inlets of the sample boxes were shortened in comparison to the NEU arrangement (I.D.=0.8 cm, length=20 cm) and a PFA Teflon gauze (instead of the mosquito net) was placed inside a home-made PFA Teflon rain protection.

#### 2.1.4 Calibration and errors of the concentration measurements

The FIA cell was calibrated using liquid standards once a week, while the IC response was checked with liquid standards once or twice during each experiment. Field blanks representing the zero concentration signal of the system were measured once a week by switching off the sampling pumps and sealing the inlets, leaving the rest of the system unchanged (see Thomas et al., 2009). The random error of the measured air concentrations of  $\text{NH}_3$ ,  $\text{HNO}_3$ ,  $\text{NH}_4^+$  and  $\text{NO}_3^-$  was calculated according to Trebs et al. (2004) and Thomas et al. (2009) using Gaussian error propagation. The concentration error depends on the individual random errors of the sample airflow, the liquid sample flow, the bromide standard concentration and the peak integration. Following suggestions by Thomas et al. (2009), the field performance of GRAEGOR was checked not only by monitoring the FIA waste flow, double-de-ionized water conductivity, and IC

## An analysis of precision requirements and flux errors

V. Wolff et al.

Title Page

Abstract

Introduction

Conclusions

References

Tables

Figures

⏪

⏩

◀

▶

Back

Close

Full Screen / Esc

Printer-friendly Version

Interactive Discussion



performance, but also by (a) measuring the air flow through the sample boxes with an independent device (Gilibrator, Gilian, Sensodyne) once per day and (b) measuring and adjusting the liquid flow supply of the SJAC once per week. Additionally, other factors may affect the sample efficiency of the sample boxes. Therefore, the coating of the denuders was visually checked at least once per day and also the inlets were checked every day for visible contamination and water droplets.

### 2.1.5 Determination of the concentration difference error

Evaluating potential error sources of the concentrations measured by GRAEGOR, it is obvious that some of them (e.g., the error of the bromide standard, see Sect. 2.2.2) do not influence the error of the difference between the concentrations,  $\sigma_{\Delta C}$ , sampled by the two individual sampling boxes because the same analytical unit and the same standard solutions are used for deriving both concentrations. Some of the error sources of an individual concentration value are, however, relevant for  $\Delta C$ , as they may theoretically impact the concentrations at the two heights differently (e.g. the airflow through the sample boxes and the liquid flows). Additionally, other factors may introduce different sample efficiency of the sample boxes and thus impact on the precision of  $\Delta C$ . Thus, the determination of  $\sigma_{\Delta C}$  is not to be performed straight forward from the error in concentrations.

Some of the factors lead to random errors, i.e. to a scatter in both directions around a “true value”, whereas some of them may lead to temporal or non-temporal systematic errors, such as constant different sampling efficiencies. In order to investigate and characterize these errors, we performed extended side-by-side measurements during our field experiments, as integrated error analysis for  $\Delta C$ . The sample boxes were regularly placed side-by-side during time periods of different length, but totally of 352 h (NEU) and of 255 h (EGER). During NEU, sampling could be performed through one common inlet at  $z=0.9$  m above ground, since the boxes were located close to the ground. During EGER, the two boxes were standing next to each other (24.4 m above ground), with a distance of 0.4 m between the inlets. During NEU, four side-by-side

## An analysis of precision requirements and flux errors

V. Wolff et al.

Title Page

Abstract

Introduction

Conclusions

References

Tables

Figures

⏪

⏩

◀

▶

Back

Close

Full Screen / Esc

Printer-friendly Version

Interactive Discussion



measurement periods were performed, while during EGER, due the difficult set up at the tower, we confined ourselves to two side-by-side measurement periods at the beginning and the end of the experiment.

We plotted the concentrations measured with the two sample boxes side-by-side against each other and made an orthogonal fit through the scatter plots by minimizing the perpendicular distances from the data to the fitted line. That way, both concentration values are treated the same way, taking into account that both concentrations may be prone to measurement errors. We define a consistent deviation from the 1:1 line as systematic difference between the concentration measurements and we correct for it applying the calculated fit-equation. We regard the remaining scatter around the fit as random error between the concentration measurements of the two boxes.

## 2.2 The aerodynamic gradient method (AGM)

Applying the AGM the turbulent vertical transport of an entity towards to or away from the surface is, in analogy to Fick's first law, considered as the product of the turbulent diffusion (transfer) coefficient and the vertical air concentration gradient  $\partial C/\partial z$  in the so-called constant flux layer (Foken, 2006).

$$F_C = -K_H(u_*, z, L) \cdot \frac{\partial C}{\partial z} \quad (1)$$

Usually, the turbulent diffusion coefficients for scalars (sensible heat, water vapour, trace compounds) are assumed to be equal (Foken, 2006). The turbulent diffusion coefficient for sensible heat,  $K_H$ , expresses both, the mechanic turbulence, induced by friction shear (expressed through the friction velocity,  $u_*$ ) and the thermal turbulence induced by the thermal stability of the atmosphere (expressed in  $z/L$ ). It is thus a function of the height  $z$  (m) above the zero plane displacement height  $d$  (m), and atmospheric stability, parameterized by the Monin-Obukhov length  $L$  (m):

$$L = -\frac{u_*^3}{\kappa \cdot \frac{g}{T} \cdot \frac{H}{\rho \cdot c_p}} \quad (2)$$

### An analysis of precision requirements and flux errors

V. Wolff et al.

Title Page

Abstract

Introduction

Conclusions

References

Tables

Figures

◀

▶

◀

▶

Back

Close

Full Screen / Esc

Printer-friendly Version

Interactive Discussion



## An analysis of precision requirements and flux errors

V. Wolff et al.

Title Page

Abstract

Introduction

Conclusions

References

Tables

Figures

◀

▶

◀

▶

Back

Close

Full Screen / Esc

Printer-friendly Version

Interactive Discussion

where  $u_*$  is the friction velocity ( $\text{m s}^{-1}$ ),  $g$  the acceleration of gravity ( $\text{m s}^{-2}$ ),  $T$  the (absolute) air temperature (K),  $H$  the turbulent sensible heat flux ( $\text{W m}^{-2}$ ),  $\rho$  the air density ( $\text{kg m}^{-3}$ ),  $c_p$  the specific heat of air at constant pressure, and  $\kappa$  the von Karman constant (0.4) (Arya, 2001).  $H$  and  $u_*$  are usually measured by the eddy-covariance technique (or derived from gradient measurements of the vertical gradients of wind speed and air temperature; Garratt, 1992).

For practical reasons, the flux-gradient relationship is usually not applied in the differential form (Eq. 1) but in an integral form between two measurement heights,  $z_1$  and  $z_2$  (in m); accordingly the flux is derived from the difference in concentration,  $\Delta C = C_2 - C_1$  (in  $\mu\text{g m}^{-3}$ ), measured at the two heights, as (Mueller et al., 1993):

$$F_C = - \frac{u_* \cdot \kappa}{\underbrace{\ln\left(\frac{z_2}{z_1}\right) - \Psi_H\left(\frac{z_2}{L}\right) + \Psi_H\left(\frac{z_1}{L}\right)}_{=v_{tr}}} \cdot \Delta C \quad (3)$$

with  $\kappa$  the von Karman constant (0.4) and  $\Psi_H$ , the integrated stability correction function for sensible heat (equal to that of trace compounds). The left term of the product on the right hand side of Eq. (3) is often referred to as the transfer velocity,  $v_{tr}$  ( $\text{m s}^{-1}$ ). It represents the inverse resistance of the turbulent transport between the two heights  $z_1$  and  $z_2$  (Ammann, 1998). Note here, that we use all measurement heights  $z_1$ ,  $z_2$ , and  $z$ , as aerodynamic heights above the zero plane displacement height,  $d$ . For the grassland site (NEU) with varying canopy height  $h_{\text{canopy}}$ ,  $d$  (in m above ground) was estimated as  $d = 0.66 \cdot (h_{\text{canopy}} - 0.06)$  according to Neftel et al. (2007), and for the forest site (with constant canopy height during our study) it was determined as 14 m above ground (Thomas and Foken, 2007).

When applying the AGM the accurate measurement of the concentration difference of the substance of interest is the major challenge. This is especially the case in remote environments, where concentrations are very low (Wesely and Hicks, 2000) and vertical concentration differences are in the order of 1 to 20% of the mean concentration

(Businger, 1986; Foken, 2006).

## 2.3 Flux error analysis

When applying the AGM for measurements of two point vertical concentration differences, the flux is determined from the product of  $\Delta C$  and  $v_{tr}$  (see Eq. 3). A flux error thus includes the errors of factors,  $\sigma_{\Delta C}$  and  $\sigma_{v_{tr}}$ .  $\sigma_{\Delta C}$  is derived from side-by-side measurements as described in Sect. 2.2.3.  $\sigma_{v_{tr}}$  will be estimated from errors of the main influencing parameters of  $v_{tr}$  as described in Sect. 4.4.

These two errors,  $\sigma_{\Delta C}$  and  $\sigma_{v_{tr}}$ , have different effects on the resulting flux, its sign, magnitude and error. The sign of  $\Delta C$  determines the sign and therefore the direction of the derived flux. Thus,  $\sigma_{\Delta C}$  is a measure of the significance of the derived flux direction, additionally to the influence of  $\sigma_{\Delta C}$  on the magnitude of the flux error. The error of  $v_{tr}$  however, expresses the uncertainty in the velocity of exchange and therefore influences the magnitude of the flux error, but  $\sigma_{v_{tr}}$  does not impact the significance of the flux sign. From  $\sigma_{\Delta C}$  we can deduce the significance of a difference from zero and subsequently of the flux direction. The error of the flux,  $\sigma_F$ , we deduce by combining the two values,  $\sigma_{\Delta C}$  and  $\sigma_{v_{tr}}$ , using Gaussian error propagation:

$$\sigma_F = F \cdot \sqrt{\left(\frac{\sigma_{v_{tr}}}{v_{tr}}\right)^2 + \left(\frac{\sigma_{\Delta C}}{\Delta C}\right)^2} \quad (4)$$

## 3 Constraints for the precision – theoretical approach

To obtain an estimate of the precision required to resolve vertical concentration gradients with regard to stability and measurement heights using Eq. (3), an independent flux estimate is necessary. For components that typically feature unidirectional deposition fluxes, such as  $\text{HNO}_3$ , the so-called inferential method may be used to obtain a maximum deposition flux estimate. The inferential method is based on the “big leaf

### An analysis of precision requirements and flux errors

V. Wolff et al.

Title Page

Abstract

Introduction

Conclusions

References

Tables

Figures

◀

▶

◀

▶

Back

Close

Full Screen / Esc

Printer-friendly Version

Interactive Discussion

## An analysis of precision requirements and flux errors

V. Wolff et al.

Title Page

Abstract

Introduction

Conclusions

References

Tables

Figures

⏪

⏩

◀

▶

Back

Close

Full Screen / Esc

Printer-friendly Version

Interactive Discussion

multiple resistance approach” (Wesely and Hicks, 2000; Hicks et al., 1987). In analogy to Ohm’s law, the flux of  $\text{HNO}_3$  is expressed as the ratio of the  $\text{HNO}_3$  concentration,  $C_{\text{HNO}_3}$  at one height and the resistances against deposition to the ground. This resistance consists of three individual resistances  $R_a$ ,  $R_b$ , and  $R_c$ , each of them characterizing part of the deposition process:

$$F_{\text{HNO}_3} = -\frac{1}{R_a + R_b + R_c} \cdot C_{\text{HNO}_3} \quad (5)$$

with  $F_{\text{HNO}_3}$  denoting the  $\text{HNO}_3$  deposition flux ( $\mu\text{g m}^{-2} \text{s}^{-1}$ ),  $R_a$  the aerodynamic resistance ( $\text{s m}^{-1}$ ),  $R_b$  the quasi-laminar or viscous boundary layer resistance ( $\text{s m}^{-1}$ ),  $R_c$  the surface resistance ( $\text{s m}^{-1}$ ) and  $C_{\text{HNO}_3}$  the concentration of  $\text{HNO}_3$  ( $\mu\text{g m}^{-3}$ ).  $R_a$  is calculated according to Garland (1977). It is defined for a measurement height  $z$  (m) above a surface of roughness length  $z_0$  (m):

$$R_a(z, z_0) = \frac{1}{\kappa \cdot u_*} \left[ \ln \left( \frac{z}{z_0} \right) - \Psi_H \left( \frac{z}{L} \right) \right] \quad (6)$$

The roughness length,  $z_0$ , of the grassland site was derived from wind and turbulence measurements (Neffel et al., 2007) as a function of the canopy height:  $z_0 = 0.25 \cdot (h_{\text{canopy}} - d)$ . Wind profile analysis for the forest site revealed a value of  $z_0$  of 2 m (Thomas and Foken, 2007).  $R_b$  determines the exchange immediately above the vegetation elements and can be described by (Hicks et al., 1987):

$$R_b = \frac{2}{\kappa \cdot u_*} \left( \frac{\text{Sc}}{\text{Pr}} \right)^{\frac{2}{3}} \quad (7)$$

where Sc and Pr are the Schmidt and Prandtl number ( $\approx 0.72$ ), respectively. Sc is a strong function of the molecular diffusivity of the trace gas (for  $\text{HNO}_3 \approx 1.25$ ) (Hicks et al., 1987). Due to the high surface affinity and the observed high deposition rates of  $\text{HNO}_3$ , the canopy resistance,  $R_c$ , is often assumed to be zero (e.g., Sievering et al.,

2001; Hanson and Lindberg, 1991) and thus, the theoretical maximum deposition flux of  $\text{HNO}_3$  towards the surface can be obtained by:

$$F_{\max_{\text{HNO}_3}} = -\frac{1}{R_a + R_b} \cdot C_{\text{HNO}_3} \quad (8)$$

This maximum  $\text{HNO}_3$  flux value (calculated with  $C_2$  at height  $z_2$ ) will be used to estimate the minimal requirements which the instrument's precision must satisfy to determine fluxes with the AGM at the two sites for a range of atmospheric stabilities.

### 3.1 Influence of atmospheric stability

Combining Eqs. (3) and (8) we may calculate a maximum possible concentration difference for the maximum  $\text{HNO}_3$  deposition flux ( $R_c=0$ )

$$\Delta C_{\max} = \frac{C_{\text{HNO}_3} \cdot \left[ \ln\left(\frac{z_2}{z_1}\right) - \Psi_H\left(\frac{z_2}{L}\right) + \Psi_H\left(\frac{z_1}{L}\right) \right]}{\kappa \cdot u_* \cdot [R_a(z, z_0) + R_b]} \quad (9)$$

Including Eqs. (6) and (7) and solving the equation for the maximum concentration difference relative to the  $\text{HNO}_3$  concentration, we obtain:

$$\frac{\Delta C_{\max}}{C_{\text{HNO}_3}} = \frac{\ln\left(\frac{z_2}{z_1}\right) - \Psi_H\left(\frac{z_2}{L}\right) + \Psi_H\left(\frac{z_1}{L}\right)}{\ln\left(\frac{z_2}{z_0}\right) - \Psi_H\left(\frac{z_2}{L}\right) + 2 \cdot \left(\frac{Sc}{Pr}\right)^{\frac{2}{3}}} \quad (10)$$

Equation (10) provides a minimal requirement for the instrument precision to resolve vertical concentration differences as a function of the aerodynamic stability ( $z/L$ ), the ratio of the two measurement heights ( $z_2/z_1$ ), and the roughness length of the underlying surface ( $z_0$ ). Whereas the stability generally varies strongly with the time of day, the latter two parameters are usually constant for a given site. The two field sites in this study represent contrasting conditions in this respect.

Title Page

Abstract

Introduction

Conclusions

References

Tables

Figures

⏪

⏩

◀

▶

Back

Close

Full Screen / Esc

Printer-friendly Version

Interactive Discussion



## An analysis of precision requirements and flux errors

V. Wolff et al.

Title Page

Abstract

Introduction

Conclusions

References

Tables

Figures

◀

▶

◀

▶

Back

Close

Full Screen / Esc

Printer-friendly Version

Interactive Discussion

We have calculated  $\Delta C_{\max}/C$  for a range of stabilities using the roughness length ( $z_0$ ) and the measurement heights of the two sites using different parameterisations for  $R_b$  (Fig. 2).  $\Delta C_{\max}/C$  depends to a large extent on the atmospheric stability, ranging from 55% at the grassland site for extremely stable conditions (32% at the forest site) to less than 10% at the grassland (around 5% at the forest site) for labile conditions. Higher roughness at the forest site (EGER) leads to generally lower  $\Delta C_{\max}/C$  values for all stabilities compared to the grassland site.

### 3.2 Influence of the measurement heights

The influence of the measurement heights above the surface on the minimal precision requirements is also estimated from Eq. (10). For near neutral conditions, when  $z/L$  is close to zero,  $\Psi_H$  is close to zero such that we may simplify Eq. (10) to:

$$\frac{\Delta C_{\max}}{C_{\text{HNO}_3}} = \frac{\ln\left(\frac{z_2}{z_1}\right)}{\ln\left(\frac{z_2}{z_0}\right) + 2 \cdot \left(\frac{Sc}{Pr}\right)^{\frac{2}{3}}} \quad (11)$$

The second term in the denominator is a constant derived from  $R_b$ , which has a bigger influence on  $\Delta C_{\max}/C$  above a forest than above grassland, where  $\ln(z_2/z_0)$  is smaller.  $\Delta C_{\max}/C$  increases with increasing  $z_2/z_1$  values (Fig. 3), thus the precision requirements decrease with increasing measurement height ratios. There are, however, restrictions to the choice of measurement heights. The upper measurement height must be chosen according to fetch limitations, i.e. the uniform fetch length must be larger than one hundred times the measurement height (e.g. Businger, 1986). Above forests, the tower height and the sensor accessibility are additional limiting factors. In turn, the position of the lower inlet height, which might be chosen as low as possible to maximize the ratio  $z_2/z_1$ , is limited by other micrometeorological issues like the roughness sublayer and internal boundary layers. According to fetch limitations and site characteristics, the measurement height ratios during our studies were 3.4 and 1.6 (NEU and

EGER), respectively.

Above rough surfaces, such as forest canopies, deviations from the ideal flux-gradient relationship used here are frequently observed within the so-called roughness sublayer, which may extend up to two times the canopy height (Foken, 2006). In this layer the use of flux gradient relations may underestimate scalar fluxes by 10% or more (Simpson et al., 1998; Thom et al., 1975; Hogstrom, 1990; Garratt, 1978; Cellier and Brunet, 1992). Therefore the detection limits for EGER derived here have to be considered as rough estimates. A detailed analysis of the site-specific flux-profile relationships above the forest (derived for non-reactive trace gases) will be published elsewhere.

## 4 Experimental results

### 4.1 Overview

The determined random error of the measured air concentrations, determined after Trebs et al. (2004) and Thomas et al. (2009), was in the order of 10%. Note here, that only individual quantifiable error sources are included in this error estimation. Errors in concentration values that are not quantifiable, e.g. errors due to limited sampling efficiency, may only be investigated by differential analysis, like the side-by-side measurements (see Sects. 2.2.3 and 4.2). The limit of detection (LOD) under field conditions was determined as three times the standard deviation of the blank values (Kaiser and Specker, 1956) and results are summarized in Table 1. During NEU, problems with the membrane in the FIA and sensor damage in the course of the experiment increased the LOD of the  $\text{NH}_3/\text{NH}_4^+$ -measurement.

Concentration values below the detection limit were used in the general time series analysis, but data points were flagged and their error ( $\sigma_C/C$ ) was set to 100%. However, for the side-by-side evaluation they were excluded. Furthermore, data points were excluded from further analysis based on chromatogram quality, water quality, air

## An analysis of precision requirements and flux errors

V. Wolff et al.

Title Page

Abstract

Introduction

Conclusions

References

Tables

Figures

⏪

⏩

◀

▶

Back

Close

Full Screen / Esc

Printer-friendly Version

Interactive Discussion

and liquid flow stability and obvious contamination (e.g. after manual air flow measurement). An outlier test was performed according to Vickers and Mahrt (1997) and the respective values were excluded from analysis. The overall data availability during the experiments is shown in Table 2. Roughly 10% of the measurement period was used for calibrations and blanks. One third was used for side-by-side measurements and two thirds of the measurement period the instrument measured concentration at two different heights.

## 4.2 Diel variation of concentrations and aerodynamic parameters

Diel variations of the concentrations measured during the experiments are presented in Fig. 4 (NEU) and Fig. 5 (EGER) as median, 0.25 and 0.75 percentiles. During NEU,  $\text{NH}_3$  concentrations at  $z=0.37$  m (above ground) (median values:  $1.24$  to  $3 \mu\text{g m}^{-3}$ ) exceeded concentrations of all other compounds by a factor of 2 to 4 and were higher than those observed during EGER (median values:  $0.46$  to  $1.16 \mu\text{g m}^{-3}$ ). During NEU,  $\text{NH}_3$  concentrations featured a sharp peak during the morning hours, while  $\text{NH}_3$  peaked in the afternoon/late afternoon hours during EGER. Concentrations of particulate  $\text{NH}_4^+$  were twice as high during EGER (median values:  $0.9$  to  $1.44 \mu\text{g m}^{-3}$ ) compared to NEU (median values:  $0.31$  to  $0.77 \mu\text{g m}^{-3}$ ). During both campaigns, particulate  $\text{NH}_4^+$  exhibited a diel variation with higher concentrations during nighttime and lower concentrations during daytime.  $\text{HNO}_3$  concentration levels were similar during NEU and EGER with median values between  $0.2$  and  $0.7 \mu\text{g m}^{-3}$ . No significant diel variation of  $\text{HNO}_3$  was observed above the forest during EGER while  $\text{HNO}_3$  featured a typical diel cycle with broad maxima in the afternoon during NEU. Particulate  $\text{NO}_3^-$  concentrations were much larger during EGER than during NEU, with median values between  $1.8$  and  $3 \mu\text{g m}^{-3}$ . Although, the variation of particulate  $\text{NO}_3^-$  was smaller during EGER than during NEU, it typically showed highest values during nighttime and/or in the early morning hours.

The friction velocity,  $u_{*}$ , ranged between  $0.07$  and  $0.23 \text{ m s}^{-1}$  during NEU, with high-

## An analysis of precision requirements and flux errors

V. Wolff et al.

Title Page

Abstract

Introduction

Conclusions

References

Tables

Figures

⏪

⏩

◀

▶

Back

Close

Full Screen / Esc

Printer-friendly Version

Interactive Discussion

**An analysis of  
precision  
requirements and  
flux errors**

V. Wolff et al.

est values during the day (Fig. 6).  $z/L$  ranged from  $-0.25$  to  $0.3$ , indicating stable conditions at night and unstable and near neutral conditions during the day. During EGER,  $u_*$  was much higher with values between  $0.25$  and  $0.8 \text{ m s}^{-1}$  and  $z/L$  was between  $-0.3$  and  $0.5$ , also indicating stable conditions during nighttime and neutral/unstable conditions during daytime.

A detailed analysis of the data acquired during NEU and EGER including gas-particle interactions and flux interpretations will be performed in subsequent publications.

**4.3 Error of  $\Delta C$  determined from side-by-side measurements**

To estimate the effective error of  $\Delta C$  ( $\sigma_{\Delta C}$ ) under field conditions, we used results from extended side-by-side sampling periods during both experiments. The weather conditions and ambient concentrations of the compounds under study were similar during side-by-side and aerodynamic gradient measurements. Results from the side-by-side measurements are displayed as scatter plots in Figs. 7 and 8 for NEU and for EGER, respectively. Concentrations sampled during rain events and during episodes with high relative humidity ( $>95\%$ ) are excluded from the side-by-side evaluation and from the flux determinations, since during these times adsorption processes in the humid inlet and potential contamination of the denuder by water droplets can not entirely be excluded.

Figures 7 and 8 show marked linear correlations between concentrations measured by the two sample boxes, however, deviations from the 1:1 line and scatter around the fitted lines is visible.  $\text{HNO}_3$  side-by-side measurements featured slopes with little deviation from the 1:1 line (1.01 and 1.02 for NEU and EGER, respectively) and small offsets. Side-by-side measurements for  $\text{NH}_3$  during NEU (Fig. 7a) also featured a slope close to unity (slope: 0.93). During EGER (Fig. 8a), under much lower  $\text{NH}_3$  concentrations, the deviation from the 1:1 line was somewhat larger (1.13), whereas the offset was smaller. For the particulate compounds ( $\text{NH}_4^+$  and  $\text{NO}_3^-$ ) the deviations from the 1:1 line are larger than for  $\text{HNO}_3$  and  $\text{NH}_3$  (Figs. 7b,d and 8b,d). The largest deviation from the 1:1 line in both experiments is observed for particulate  $\text{NH}_4^+$ , with

Title Page

Abstract

Introduction

Conclusions

References

Tables

Figures

◀

▶

◀

▶

Back

Close

Full Screen / Esc

Printer-friendly Version

Interactive Discussion



a slope of 1.59 in the NEU experiment and 1.31 in the EGER experiment.

After we corrected the data using the orthogonal fit (systematic deviation, see above), the remaining scatter around the fit (the residuals) was used to determine  $\sigma_{\Delta C}$ . Figure 9 shows exemplarily two typical residual distributions.

The histograms of the residuals show a pronounced peak around zero with a steep decrease of the relative frequency and pronounced tails towards both directions (increasing residuals of  $\Delta C$ ). These distributions follow more closely a Laplace (or double exponential) distribution than a Gaussian distribution, as it was also observed for errors in the measurements of other atmospheric quantities (Richardson et al., 2006). In contrast to the usual Gaussian distribution, the standard deviation (1std) of values following the Laplace distribution is determined as:

$$\text{std}_{\text{Laplace}} = \sqrt{2} \cdot \frac{\sum_{i=1}^N |x_i - \bar{x}|}{n} \quad (12)$$

with  $n$  denoting the total number of values within the distribution,  $\bar{x}$  the mean, and  $x_i$  all residual values, which encompass 76% of the Laplace distribution (which corresponds to 68.27% in the Gaussian distribution, analogously, 2std correspond to 95.45% of a Gaussian distribution, but to 94% of a Laplace distribution; see Richardson et al., 2006).

The distributions of concentration residuals provide valuable information on the behaviour of the instrument. The width of the residual distribution characterizes the random concentration difference during side-by-side measurements in the field. The Laplace standard deviations for each of the compounds are given in Table 3 for the two experiments. For comparison, the standard deviations calculated for the Gaussian distribution are also shown.

For  $\text{NH}_3$ ,  $\text{HNO}_3$  and  $\text{NO}_3^-$  during NEU and  $\text{NH}_3$ ,  $\text{NH}_4^+$  and  $\text{HNO}_3$  during EGER, we observed increasing  $\text{std}_{\Delta C}$  values with increasing  $C$ . Therefore, we plotted  $\text{std}_{\Delta C}$  vs.  $C$  measured by SB2 and made a linear regression (see Figs. 10 and 11), which can be

## An analysis of precision requirements and flux errors

V. Wolff et al.

Title Page

Abstract

Introduction

Conclusions

References

Tables

Figures

◀

▶

◀

▶

Back

Close

Full Screen / Esc

Printer-friendly Version

Interactive Discussion

**An analysis of  
precision  
requirements and  
flux errors**

V. Wolff et al.

Title Page

Abstract

Introduction

Conclusions

References

Tables

Figures

⏪

⏩

◀

▶

Back

Close

Full Screen / Esc

Printer-friendly Version

Interactive Discussion

used to determine  $\text{std}_{\Delta C}$  as a function of  $C$ . The relative values  $\text{std}_{\Delta C}/C$  derived from the slopes of the regressions, which are used as estimates of  $\sigma_{\Delta C}$ , are summarized in Table 4. For particulate  $\text{NH}_4^+$  during NEU and for particulate  $\text{NO}_3^-$  during EGER, this approach did not appear to be useful, because the residuals did not show a clear dependence on  $C$  in these cases. Hence, we defined the overall Laplace standard deviation (Table 3) as the error  $\sigma_{\Delta C}$ . Median relative determined errors ( $\sigma_{\Delta C}/\Delta C$ ) were 36.3 and 55.5% for  $\text{NH}_3$ , 40.1 and 59.4% for  $\text{HNO}_3$ , 129.6 and 63.3% for particulate  $\text{NH}_4^+$  and 49.4 and 244% for particulate  $\text{NO}_3^-$  during NEU and EGER, respectively.

The resulting  $\sigma_{\Delta C}$  values may be used for two purposes: (a) to describe an uncertainty range around zero, and thus give an estimate about the precision of the gradient system at a given concentration, and (b) to determine the significance of a measured  $\Delta C$  value for flux calculations.  $\Delta C$  values inside the uncertainty range around zero carry error bars that are larger than  $\Delta C$  itself and it is not possible to derive significant fluxes from these  $\Delta C$  values, nor meaningful deposition velocities.

We define those  $\Delta C$  values as insignificantly different from zero. Results of this analysis for some days of the EGER experiment are displayed in Fig. 12. In cases when the uncertainty range is a function of concentration, the diel variation of concentrations is reflected in the size of the error bars and uncertainty ranges (grey bars). For example, for  $\text{NH}_3$  concentrations during EGER error bars are larger during daytime when  $\text{NH}_3$  concentrations are high (Fig. 12a). For the days shown here, both, significant and non-significant  $\Delta C$  values are observed.

From the relative values,  $\sigma_{\Delta C}/C$ , in Table 4 we define an uncertainty range around zero and therefore a significance level for  $\Delta C$  for the given ambient concentration. Between 11 to 54% of the individual  $\Delta C$  values, determined from aerodynamic gradient measurements, during EGER and NEU are found to be significantly different from zero (Table 5).

#### 4.4 Error of the transfer velocity

Since the exchange flux of the considered trace gases is defined as the product of  $\Delta C$  and  $v_{tr}$  we also need to investigate  $\sigma_{v_{tr}}$ . As stated above,  $v_{tr}$  is a function of  $u_*$ , and, in the denominator,  $\ln(z_2/z_1)$  and the integrated stability correction functions for heat (=trace compounds) for both measurement heights ( $\Psi_H(z_1/L)$  and  $\Psi_H(z_2/L)$ ), which are (via the Monin-Obukhov length, Eq. 2) a function of  $u_*$ , the sensible heat flux ( $H$ ), a buoyancy parameter ( $g/T$ ), the air density ( $\rho$ ), the von Karman constant and the specific heat ( $c_p$ ) (e.g., Arya 2001).

A complete error analysis of  $v_{tr}$  would require information about the error of all these parameters. We have not found any study, which has thoroughly quantified  $\sigma_{v_{tr}}$ . Since a detailed analysis of  $\sigma_{v_{tr}}$  is not the main scope of this study, we use a simplified approach to estimate this value. A first simple approach is to scale the error of the transfer velocity with the error of  $u_*$ , especially under near-neutral conditions, when the integrated empirical functions in the denominator of Eq. (3) approach unity. For the sonic anemometer used during our studies, the error of  $u_*$  can be estimated as  $\leq 10\%$  (Foken, 2006). This relative error would directly propagate to  $v_{tr}$ .

For non-neutral conditions, error estimates of the empirical functions within the stability range of  $-0.5 \leq z/L \leq +0.5$  exist (Foken, 2006). Assuming that the errors remain the same when integrating the empirical functions the errors would also be in the range of  $\leq 10\%$ . Assuming near-normal distribution of both  $\sigma_{u_*}$  and  $\sigma_{\Psi_H}$ ,  $\sigma_{v_{tr}}$  can be calculated according to:

$$\frac{\sigma_{v_{tr}}}{v_{tr}} = \pm \sqrt{\left(\frac{\sigma_{u_*}}{u_*}\right)^2 + \left(\frac{\sigma_{\Psi_H}}{\Psi_H}\right)^2 \cdot \left(\frac{(\Psi_H(z_2) + \Psi_H(z_1))^2}{\left(\ln\left(\frac{z_2}{z_1}\right) - \Psi_H(z_2) + \Psi_H(z_1)\right)^2}\right)} \quad (13)$$

The right hand term of the product under the square root accounts for the fact that in Eq. (3) two  $\Psi_H$  functions appear in the denominator. Note that we assume a maximum relative error of both  $\Psi_H$  functions (10%). The errors of  $u_*$  and  $\Psi_H$  add up to a daytime

Title Page

Abstract

Introduction

Conclusions

References

Tables

Figures

◀

▶

◀

▶

Back

Close

Full Screen / Esc

Printer-friendly Version

Interactive Discussion



( $-0.5 \leq z/L \leq +0.5$ )  $\sigma_{v_{tr}}/v_{tr}$  of around 10% (median) during NEU (inter-quartile range: 10.1–13.3%) and 13% (median) during EGER (inter-quartile range: 10.3–23.2%). Note that for small  $u_*$  values, the assumption of a constant relative error may not be appropriate.

## 4.5 Flux error

In the previous sections we have determined  $\sigma_{\Delta C}/C$  and we also obtained an error estimate for  $\sigma_{v_{tr}}/v_{tr}$ . We combine these relative errors and derive the flux error,  $\sigma_F$ , applying Eq. (4). The resulting  $\sigma_F$  are presented along with determined fluxes in Fig. 13 for some days during EGER.

Most of the time  $\sigma_F$  is primarily governed by  $\sigma_{\Delta C}$ , but on the 22 and 23 September, large  $\sigma_{v_{tr}}$  values dominate  $\sigma_F$  during daytime. The overall  $\sigma_F$  during EGER would decrease by 4% (median, inter-quartile range: 2–10%) if we exclude  $\sigma_{v_{tr}}$  and use  $\sigma_{\Delta C}$  only. During NEU, the error would decrease by 2% (median, inter-quartile range: 1–4%). It is evident that,  $\sigma_F$  depends to a major extent on the capability of the instrument to precisely resolve vertical concentration differences.

The statistical distribution of flux errors relative to the determined flux values ( $\sigma_F/F$ ) for  $\Delta C$  values larger than  $\sigma_{\Delta C}$  are presented in Fig. 14 for NEU and Fig. 15 for EGER. Medians of  $\sigma_F/F$  vary between 31 and 68%. The values are comparable for all compounds, but show slightly larger ranges and higher medians for  $\text{NH}_4^+$  during NEU and  $\text{NO}_3^-$  during EGER

## 5 Discussion

### 5.1 Side-by-side performance of the GREAGOR system

As stated in Sect. 2.2.3 the error in concentration difference,  $\sigma_{\Delta C}$ , may not be derived from the error in concentrations, as some of the factors that influence  $C$  do not impact

## An analysis of precision requirements and flux errors

V. Wolff et al.

Title Page

Abstract

Introduction

Conclusions

References

Tables

Figures

⏪

⏩

◀

▶

Back

Close

Full Screen / Esc

Printer-friendly Version

Interactive Discussion

---

**An analysis of  
precision  
requirements and  
flux errors**V. Wolff et al.

---

[Title Page](#)[Abstract](#)[Introduction](#)[Conclusions](#)[References](#)[Tables](#)[Figures](#)[⏪](#)[⏩](#)[◀](#)[▶](#)[Back](#)[Close](#)[Full Screen / Esc](#)[Printer-friendly Version](#)[Interactive Discussion](#)

on  $\Delta C$ , but others do. The error of the peak integration, which affects the measured liquid concentration and the measured bromide concentration (cf. Trebs et al., 2004), for example, is relevant for  $\Delta C$  as these errors may vary during the sequential runs of the ion chromatograph. Additionally, the two airflows through the sample boxes may have slightly different variations since the two critical orifices are not entirely identical. There are also some other factors that may affect  $\Delta C$  which are hard to quantify and to monitor. The wet-annular rotating denuder walls may not always be perfectly coated, and the liquid levels, controlled by optical sensors, may be slightly different between the two wet-annular rotating denuders. The difference in coating quality would lead to slightly different sampling efficiencies between the two heights, especially if the coating is not perfect in the first part of the denuder (Thomas et al., 2009). The difference in water level results in a different response time of the instrument, leading to a dampening of concentration variations in the potentially affected denuder (Thomas et al., 2009).  $\Delta C$  may also be influenced by inlet effects of the two sample boxes. Due to their high solubility and high surface affinity,  $\text{HNO}_3$  and  $\text{NH}_3$  may be lost in the inlet, especially under very humid conditions. To minimize these effects we used short PFA tubing and treat measurement values from periods with rain and high relative humidity with caution. This, however, may not fully exclude different behaviour of the two inlets.

The discussed error sources have different effects on the sampled species, which is most evident for particulate  $\text{NH}_4^+$ . Sorooshian et al. (2006) showed that particulate  $\text{NH}_4^+$  is most vulnerable to evaporational loss within the condensation chamber of the PILS (particle into liquid sampler), whose principle of operation is comparable to the SJAC. They showed that the particulate  $\text{NH}_4^+$  sampling efficiency is dependent on the temperature of the water vapour, the pH of the sampled particulate, and the dilution. Particulate  $\text{NH}_4^+$  evaporation increases (and is therefore lost within the sample) with increasing pH and decreasing dilution. Sorooshioan et al. also showed that in contrast to particulate  $\text{NH}_4^+$  the loss of  $\text{NO}_3^-$  and  $\text{Cl}^-$  in their condensation chamber is smaller than 1%. The SJACs do not reveal this effect for higher particulate  $\text{NH}_4^+$  concentrations (see Thomas et al., 2009), but the effect appears to be consistently ob-

served for concentrations below  $2.5 \mu\text{g m}^{-3}$ . The deviation of up to 59% (Figs. 7 and 8) between the two sample boxes, suggest that the SJAC sampling efficiency was not equal for the two devices. For the NEU experiment,  $\text{NH}_4^+$  concentrations were quite low (up to  $2 \mu\text{g m}^{-3}$ ; compared to  $14 \mu\text{g m}^{-3}$  in Thomas et al., 2009) and regression was calculated for a number of only 17 data pairs. This may explain the somewhat poor side-by-side results for  $\text{NH}_4^+$  during NEU (Fig. 7).

We were not able to clarify the reasons for this behaviour yet, but since the differences proved to be quite stable during both experiments, we were able to correct for this systematic difference (cf. Sect. 2.2.3).

## 5.2 Comparison to previous studies

### 5.2.1 Overview of $\text{NH}_3$ - $\text{HNO}_3$ - $\text{NH}_4\text{NO}_3$ aerodynamic gradient measurements

Table 6 shows a list of studies that have measured and investigated vertical concentration gradients of  $\text{NH}_3$ ,  $\text{HNO}_3$  and particulate  $\text{NH}_4^+/\text{NO}_3^-$  to determine surface-atmosphere exchange fluxes over different ecosystems.

The studies with non-continuous or semi-continuous measurements were performed with denuders or filter-packs and measured integrated replicates at every measurement height. Corresponding concentration data, i.e. means and standard deviations, were then used to distinguish significant from insignificant  $\Delta C$ . In some studies precision analysis was performed by individual side-by-side measurements of denuders or filter-packs (e.g., Huebert and Robert, 1985). Resulting errors of the exchange fluxes were often only qualitatively discussed (e.g., Duyzer, 1994). Fifteen out of the twenty-eight studies made continuous or semi-continuous measurements of at least one compound in the triad (e.g. study 4, 10, and 11, Table 6), even less made measurements of the complete  $\text{NH}_3$ - $\text{HNO}_3$ - $\text{NH}_4\text{NO}_3$  triad (studies 15, 22–24 and 27, Table 6). Methods with a higher temporal resolution than the GRAEGOR can make use of several measurements within a 30 min interval to estimate random deviations and

Title Page

Abstract

Introduction

Conclusions

References

Tables

Figures

⏪

⏩

◀

▶

Back

Close

Full Screen / Esc

Printer-friendly Version

Interactive Discussion

errors (Flechard and Fowler, 1998). In contrast, a precision analysis of aerodynamic gradient measurements with longer sampling periods (e.g. 30 min like GRAEGOR) has to be performed differently, because only one concentration measurement per height per half an hour is available. Wyers et al. (1992), Wyers et al. (1993), and Kruit et al. (2007) demonstrated the use of side-by-side measurements to estimate the precision of their semi-continuous  $\text{NH}_3$  aerodynamic gradient measurements. They called deviations from the 1:1 line systematic differences and corrected for them; the standard deviation of the remaining scatter was used as an estimate of measurement noise. Many of the remaining studies do not show error estimates of their derived fluxes and deposition velocities. So far, only Thomas et al. (2009) feature a precision analysis for the whole  $\text{NH}_3$ - $\text{HNO}_3$ - $\text{NH}_4\text{NO}_3$  triad.

### 5.2.2 Error of concentration differences

About 49% of  $\Delta C$  data for  $\text{NH}_3$  during EGER were found to be not significantly different from zero (Table 5). Keeping in mind that measurements were performed above forest with the expected small  $\Delta C$  values (Fig. 3), a 51% yield of significant half hourly aerodynamic gradient measurements is satisfying. Andersen et al. (1993), who measured  $\text{NH}_3$  exchange with three hourly-integrated denuder measurements on several levels above forest, were able to use less than half of the measurements for flux calculations. Wet-chemical semi-continuous methods comparable to GRAEGOR, for which the precision to resolve vertical concentration differences was determined have been presented by Wyers et al. (1993), Kruit et al. (2007), and Thomas et al. (2009). Wyers et al. tested their  $\text{NH}_3$  gradient system (AMANDA: based on three wet-annular denuders coupled to one flow injection analytical unit) for precision by side-by-side measurements. They reported average relative standard deviation of 1.9% of 42 triplicate measurements. However, they did not give any information whether these tests were made in a controlled environment or under field conditions and whether or not side-by-side measurements were conducted regularly or only once. In 2007, Kruit et al. presented an improved  $\text{NH}_3$  gradient instrument, the GRAHAM, consisting of three

## An analysis of precision requirements and flux errors

V. Wolff et al.

Title Page

Abstract

Introduction

Conclusions

References

Tables

Figures

⏪

⏩

◀

▶

Back

Close

Full Screen / Esc

Printer-friendly Version

Interactive Discussion



wet-annular denuders and one flow injection analytical unit. Improvements compared to AMANDA were a stabilized liquid flow and monitoring of the air flow through the denuders. They tested their system under laboratory conditions, feeding the three wet-annular rotating denuders simultaneously with two different standard  $\text{NH}_3$  concentrations (0 and  $8 \mu\text{g m}^{-3}$ ) over five hours and corrected for the deviations between the samples in the same way as Wyers et al. (1993) (see Sect. 4.1.1). From these tests, they conclude that their precision was at least as good as found by Wyers et al. (1993), if not better ( $<1.9\%$ ). However, these tests do neither take into account the behaviour of the measurement system and analytical unit under ambient conditions nor the dynamic changes of ambient concentrations and associated fluctuations of temperature and relative humidity during field experiments.

In 2009, Thomas et al. introduced the GRAEGOR instrument and investigated its precision by performing a side-by-side experiment in the field under ambient conditions. They calculated linear regressions through the concentration data and used the deviation of the derived slope from the 1:1 line as their precision. They found 3% for gases and 9% for particulate compounds. The use of the deviation from the 1:1 line as precision estimate (not taking into account the scatter around it) is different to the methods used by Wyers et al. (1993) and Kruit et al. (2007), who defined this a systematic error and derived their random error from the remaining scatter. However, the approach by Thomas et al. was a first attempt to estimate the instrument precision for aerodynamic gradient measurements. Thomas et al. (2009) also defined their minimum detectable flux when  $\sigma_{\Delta C}$  equals  $\Delta C$ , but they did not take into account the error of the transfer velocity. Side-by-side measurements by Thomas et al. (2009) featured smaller systematic deviations from the 1:1 line than found in our study. Concentration ranges for  $\text{NH}_3$ ,  $\text{HNO}_3$  and  $\text{NO}_3^-$  are comparable to the ones observed in our experiments, while particulate  $\text{NH}_4^+$  presented in Thomas et al. (2009) reached  $14 \mu\text{g m}^{-3}$ , which is more than 3 times of our  $\text{NH}_4^+$  concentrations. Differences in the performance of the sample boxes may be due to small changes in the set up as well as the use of different wet-annular rotating denuder or SJAC couples. It may also be strongly influ-

## An analysis of precision requirements and flux errors

V. Wolff et al.

Title Page

Abstract

Introduction

Conclusions

References

Tables

Figures

⏪

⏩

◀

▶

Back

Close

Full Screen / Esc

Printer-friendly Version

Interactive Discussion

enced by environmental conditions (see Sect. 5.1). An analysis of the Thomas et al. side-by-side data with our method results in  $\sigma_{\Delta C}/C$  median values of 4.5% for  $\text{NH}_3$ , 1.0% for  $\text{NH}_4^+$ , 4.6% for  $\text{HNO}_3$ , and 6.8% for  $\text{NO}_3^-$ . These values are lower than the ones found in our study (see Table 4) especially for particulate  $\text{NH}_4^+$ , which however revealed much higher concentrations in Thomas et al. In this study, we combined the approaches of Wyers et al. (1993), Kruit et al. (2007), and Thomas et al. (2009) by separating systematic from random effects using the scatter around the fitted line and by using side-by-side measurements in the field to account for the actual set up of the instrument and the environmental conditions encountered at the field sites. A difference to the previous studies is the use of an orthogonal fit rather than a least squares regression to evaluate the side-by-side measurements. This fit takes into account that concentration measurements of both sample boxes may be erroneous, which is a more realistic approach than defining one of the measurements as independent (Hirsch and Gilroy, 1984; Ayers, 2001; Cantrell, 2008). The median  $\sigma_{\Delta C}/\Delta C$  values range between 36% ( $\text{NH}_3$  during NEU) and 244% ( $\text{NO}_3^-$  during EGER), see Sect. 4.2. Keeping in mind, that the GRAEGOR is a semi-continuous measurement device, delivering all compounds of the triad (and more) in hourly resolution and that we use in-field data rather than laboratory test to express an in-field precision of the instrument, these precision values are certainly satisfying.

### 5.2.3 Error of surface exchange fluxes

There are only six studies that show and discuss error bars of fluxes derived from measurements applying the AGM (see Table 6). Erismann and Wyers (1993) discussed in their study on  $\text{SO}_2$  and  $\text{NH}_3$  exchange fluxes above forest that the main error source for the  $\text{NH}_3$  flux and the  $\text{NH}_3$  canopy resistance error is  $\sigma_{\Delta C}$ . They show data of  $\text{NH}_3$  fluxes and corresponding  $R_c$  values with error bars of up to 100% and higher. They suggested an error weighted approach when doing time series analysis of these data.

Thomas et al. (2009) show a figure with flux data carrying flux errors. The magnitude relative to the flux value is not discussed in detail but is estimated well within  $\pm 50\%$ .

## An analysis of precision requirements and flux errors

V. Wolff et al.

Title Page

Abstract

Introduction

Conclusions

References

Tables

Figures

◀

▶

◀

▶

Back

Close

Full Screen / Esc

Printer-friendly Version

Interactive Discussion

The same relative value is true for flux errors shown in a figure from Duyzer et al. (1994). All these errors do not include  $\sigma_{V_{tr}}$ .

The relative flux errors  $\sigma_F/F$  determined in our study, with medians between 31 and 68% (see Figs. 14 and 15), are comparable to these studies.

### 5.3 Influence of stability conditions on the precision

In Sect. 3.1 we investigated the expected magnitude of  $\Delta C$  for a range of atmospheric stabilities, assuming a maximum  $\text{HNO}_3$  deposition flux. The precision requirement is higher for the forest site (EGER) with around 10% for near neutral and less than 10% for unstable conditions. These estimates depend to a major extend on the applied parameterisation for  $R_b$  (see Fig. 2). Comparing these values with the relative precision values given in Table 4 (EGER: right side) we see that for some species the precision may not be sufficient to determine significant  $\Delta C$  above the forest for all atmospheric stabilities.

For the grassland site (NEU), the required precision falls below 10% only at  $z/L < -0.3$ . Thus, the determined precision values (left side Table 4) are sufficient to determine significant  $\Delta C$  for most atmospheric stabilities. Note, however, that the estimate presented in Sect. 3.1 is valid for a maximum deposition flux and that not all components measured here will always deposit with maximum velocity ( $R_c > 0$ ). Thus, the expected concentration differences may well be below the values given in Sect. 3.1 for compounds other than  $\text{HNO}_3$ .

### 5.4 Influence of measurement height on the precision

It is evident from Sect. 3.2, which impact the choice of the measurement heights has on the required  $\Delta C$  to be resolved. Knowing the relative precision of the instrument, for example 8% for  $\text{NH}_3$  during EGER, minimal  $z_2/z_1$  ratios to resolve differences above a surface of given roughness can be calculated. However, as it was the case for the studies conducted here, the measurement heights must be adjusted to micrometeoro-

## An analysis of precision requirements and flux errors

V. Wolff et al.

Title Page

Abstract

Introduction

Conclusions

References

Tables

Figures

⏪

⏩

◀

▶

Back

Close

Full Screen / Esc

Printer-friendly Version

Interactive Discussion

logical considerations (such as uniform fetch length).

## 6 Conclusions

In this paper we made a comprehensive precision analysis for a novel wet-chemical instrument used for aerodynamic gradient measurements of water-soluble reactive trace gases and particles (GRAEGOR; GRadient of Aerosol and Gases Online Registrator; ECN, Petten, NL) with focus on the  $\text{NH}_3$ - $\text{HNO}_3$ - $\text{NH}_4\text{NO}_3$  triad. For the first time, we present a thorough determination of errors of multi-component surface-atmosphere exchange fluxes for two contrasting ecosystems (managed grassland and spruce forest). From our investigations, we draw conclusions on the significance of measured concentration differences and, thus, the direction and magnitude of multi-component surface-atmosphere exchange fluxes.

Additionally, we investigated theoretical minimal precision requirements for surfaces with different roughness with regard to atmospheric stability and measurement heights, which may be used for future experimental designs, knowing the precision of the instrument that will be used. Derived in-field precision values ( $\sigma_{\Delta C}/C$ ) of the instrument during our field studies were 6% (NEU, grassland) and 8% (EGER, forest) for  $\text{NH}_3$ , 6% (NEU) and 10% (EGER) for  $\text{HNO}_3$ , and 7% for particulate  $\text{NH}_4^+$  (EGER) and 5% for particulate  $\text{NO}_3^-$  (NEU). Thus, GRAEGOR is capable of resolving vertical concentration differences of the four species under investigation above grassland and forest sites for most of the prevailing atmospheric stabilities. However, our analysis revealed that, especially at the forest site, the precision of the instrument may not be sufficient to resolve individual (hourly) gradients at labile atmospheric stability, even if the substance is deposited at maximum possible speed.

Despite the fact that GRAEGOR is operated using the same analytical device for both measurement heights the median error of the determined concentration difference ranges between 36 and more than 100%. The individual errors that lead to these uncertainties are hard to quantify under field conditions. However, the determination of the

## An analysis of precision requirements and flux errors

V. Wolff et al.

Title Page

Abstract

Introduction

Conclusions

References

Tables

Figures

◀

▶

◀

▶

Back

Close

Full Screen / Esc

Printer-friendly Version

Interactive Discussion

limit of detection and side-by-side measurements under field conditions are a suitable tool to evaluate the instrument performance and to estimate the instrument precision and associated flux errors. The precision of GRAEGOR may be improved by intensive monitoring and controlling of error sources for aerodynamic gradient measurements like denuder liquid level and sample efficiency of the SJACs. We may assume that errors in previous studies, where the aerodynamic gradient method was used to derive exchange fluxes of the  $\text{NH}_3$ - $\text{HNO}_3$ - $\text{NH}_4\text{NO}_3$  triad, were at least as high as during our study, especially if two different analytical devices were applied.

The instrument provides a semi-continuous data set, constituting valuable information for mechanistic process studies. Our results form the basis to explore the errors of deposition velocities and canopy compensation point concentration, which are key-parameters used in all atmospheric chemistry and transport models. The results from the NEU and EGER campaigns will be discussed and interpreted in separate publications.

*Acknowledgements.* The authors gratefully acknowledge financial support by the European Commission (NitroEurope-IP, project 017841), the German Science foundation (DFG project EGER, ME 2100/4-1) and by the Max Planck Society. The authors wish to thank the Agroscope Reckenholz-Tänikon Research Station (ART, Air Pollution and Climate Research Group) for hosting us during the NitroEurope study and the University of Bayreuth (Micrometeorology Department) for hosting us during the EGER study.

The service charges for this open access publication have been covered by the Max Planck Society.

## An analysis of precision requirements and flux errors

V. Wolff et al.

Title Page

Abstract

Introduction

Conclusions

References

Tables

Figures

⏪

⏩

◀

▶

Back

Close

Full Screen / Esc

Printer-friendly Version

Interactive Discussion

## References

- Alsheimer, M.: Charakterisierung räumlicher und zeitlicher Heterogenitäten der Transpiration unterschiedlicher montaner Fichtenbestände durch Xylemflussmessungen, Bayreuther Forum Ökologie, 1–143, 1997.
- 5 Ammann, C.: On the Applicability of Relaxed Eddy Accumulation and Common Methods for Measuring for Measuring Trace Gas Fluxes, PhD, Geographisches Institut, ETH, Zürich, 229 pp., 1998.
- Ammann, C., Flechard, C. R., Leifeld, J., Neftel, A., and Fuhrer, J.: The carbon budget of newly established temperate grassland depends on management intensity, *Agr. Ecosyst. Environ.*, 10 121, 5–20, 2007.
- Andersen, H. V., Hovmand, M. F., Hummelshoj, P., and Jensen, N. O.: Measurements of ammonia flux to a spruce stand in Denmark, *Atmos. Environ. A Gen. Top.*, 27, 189–202, 1993.
- Andersen, H. V. and Hovmand, M. F.: Ammonia and nitric acid dry deposition and throughfall, *Water Air Soil Pollut.*, 85, 2211–2216, 1995.
- 15 Andersen, H. V., Hovmand, M. F., Hummelshoj, P., and Jensen, N. O.: Measurements of ammonia concentrations, fluxes and dry deposition velocities to a spruce forest 1991–1995, *Atmos. Environ.*, 33, 1367–1383, 1999.
- Arya, S. P.: Introduction to Micrometeorology, 2nd ed., International geophysics series, edited by: Dmoswska, R., Holton, J. R., and Rossby, H. T., Academic Press, 2001.
- 20 Ayers, G. P.: Comment on regression analysis of air quality data, *Atmos. Environ.*, 35, 2423–2425, 2001.
- Brodeur, J. J., Warland, J. S., Staebler, R. M., and Wagner-Riddle, C.: Technical note: Laboratory evaluation of a tunable diode laser system for eddy covariance measurements of ammonia flux, *Agr. Forest Meteorol.*, 149, 385–391, 2009.
- 25 Businger, J. A.: Evaluation of the accuracy with which dry deposition can be measured with current micrometeorological techniques, *J. Climate Appl. Meteorol.*, 25, 1100–1124, 1986.
- Businger, J. A. and Delany, A. C.: Chemical sensor resolution required for measuring surface fluxes by 3 common micrometeorological techniques, *J. Atmos. Chem.*, 10, 399–410, 1990.
- Calvert, J. G., Lazrus, A., Kok, G. L., Heikes, B. G., Walega, J. G., Lind, J., and Cantrell, C. A.: 30 Chemical mechanisms of acid generation in the troposphere, *Nature*, 317, 27–35, 1985.
- Cantrell, C. A.: Technical Note: Review of methods for linear least-squares fitting of data and application to atmospheric chemistry problems, *Atmos. Chem. Phys.*, 8, 5477–5487, 2008,

## An analysis of precision requirements and flux errors

V. Wolff et al.

Title Page

Abstract

Introduction

Conclusions

References

Tables

Figures

◀

▶

◀

▶

Back

Close

Full Screen / Esc

Printer-friendly Version

Interactive Discussion

<http://www.atmos-chem-phys.net/8/5477/2008/>.

Cape, J. N., van der Eerden, L. J., Sheppard, L. J., Leith, I. D., and Sutton, M. A.: Evidence for changing the critical level for ammonia, *Environ. Pollut.*, 157, 1033–1037, 2009.

Cellier, P. and Brunet, Y.: Flux gradient relationships above tall plant canopies, *Agr. Forest Meteorol.*, 58, 93–117, 1992.

Duyzer, J.: Dry deposition of ammonia and ammonium aerosols over heathland, *J. Geophys. Res.-Atmos.*, 99, 18757–18763, 1994.

Duyzer, J. H., Verhagen, H. L. M., Weststrate, J. H., and Bosveld, F. C.: Measurement of the dry deposition flux of  $\text{NH}_3$  on to coniferous forest, *Environ. Pollut.*, 75, 3–13, 1992.

Erismann, J. W., Vermetten, A. W. M., Asman, W. A. H., Waijersijpelaan, A., and Slanina, J.: Vertical-distribution of gases and aerosols – the behavior of ammonia and related components in the lower atmosphere, *Atmos. Environ.*, 22, 1153–1160, 1988.

Erismann, J. W. and Wyers, G. P.: Continuous measurements of surface exchange of  $\text{SO}_2$  and  $\text{NH}_3$  – Implications for their possible interaction in the deposition process, *Atmos. Environ. A Gen. Top.*, 27, 1937–1949, 1993.

Erismann, J. W., Draaijers, G., Duyzer, J., Hofschreuder, P., VanLeeuwen, N., Romer, F., Ruijgrok, W., Wyers, P., and Gallagher, M.: Particle deposition to forests – Summary of results and application, *Atmos. Environ.*, 31, 321–332, 1997.

Erismann, J. W. and Schaap, M.: The need for ammonia abatement with respect to secondary PM reductions in Europe, *Environ. Pollut.*, 129, 159–163, 2004.

Erismann, J. W., Bleeker, A., Hensen, A., and Vermeulen, A.: Agricultural air quality in Europe and the future perspectives, *Atmos. Environ.*, 42, 3209–3217, 2008.

Falge, E., Reth, S., Bruggemann, N., Butterbach-Bahl, K., Goldberg, V., Oltchev, A., Schaaf, S., Spindler, G., Stiller, B., Queck, R., Kostner, B., and Bernhofer, C.: Comparison of surface energy exchange models with eddy flux data in forest and grassland ecosystems of Germany, *Ecol. Model.*, 188, 174–216, 2005.

Farmer, D. K., Wooldridge, P. J., and Cohen, R. C.: Application of thermal-dissociation laser induced fluorescence (TD-LIF) to measurement of  $\text{HNO}_3$ ,  $\Sigma$  alkyl nitrates,  $\Sigma$  peroxy nitrates, and  $\text{NO}_2$  fluxes using eddy covariance, *Atmos. Chem. Phys.*, 6, 3471–3486, 2006, <http://www.atmos-chem-phys.net/6/3471/2006/>.

Flechard, C. R. and Fowler, D.: Atmospheric ammonia at a moorland site. II: Long-term surface-atmosphere micrometeorological flux measurements, *Q. J. Roy. Meteorol. Soc.*, 124, 759–791, 1998.

## An analysis of precision requirements and flux errors

V. Wolff et al.

Title Page

Abstract

Introduction

Conclusions

References

Tables

Figures

⏪

⏩

◀

▶

Back

Close

Full Screen / Esc

Printer-friendly Version

Interactive Discussion

**An analysis of  
precision  
requirements and  
flux errors**

V. Wolff et al.

[Title Page](#)[Abstract](#)[Introduction](#)[Conclusions](#)[References](#)[Tables](#)[Figures](#)[⏪](#)[⏩](#)[◀](#)[▶](#)[Back](#)[Close](#)[Full Screen / Esc](#)[Printer-friendly Version](#)[Interactive Discussion](#)

Flechard, C. R., Neftel, A., Jocher, M., Ammann, C., and Fuhrer, J.: Bi-directional soil/atmosphere N<sub>2</sub>O exchange over two mown grassland systems with contrasting management practices, *Global Change Biol.*, 11, 2114–2127, 2005.

Foken, T.: Lufthygienisch-bioklimatische Kennzeichnung des oberen Egertales (Fichtelgebirge bis Karlovy Vary), *Bayreuther Forum Ökologie*, 1–70, 2003.

Foken, T.: *Angewandte Meteorologie*, 2nd edn., Springer, 2006.

Galloway, J. N., Dentener, F. J., Capone, D. G., Boyer, E. W., Howarth, R. W., Seitzinger, S. P., Asner, G. P., Cleveland, C. C., Green, P. A., Holland, E. A., Karl, D. M., Michaels, A. F., Porter, J. H., Townsend, A. R., and Vorosmarty, C. J.: Nitrogen cycles: past, present, and future, *Biogeochemistry*, 70, 153–226, 2004.

Garland, J. A.: The dry deposition of sulphur dioxide to land and water surfaces, *Proc. R. Soc. London*, 245–268, 1977.

Garratt, J. R.: Flux profile relations above tall vegetation, *Q. J. Roy. Meteorol. Soc.*, 104, 199–211, 1978.

Garratt, J. R.: *The Atmospheric Boundary Layer*, Cambridge University Press, 1992.

Hanson, P. J. and Lindberg, S. E.: Dry deposition of reactive nitrogen compounds: A review of leaf, canopy and non-foliar measurements, *Atmos. Environ. A Gen. Top.*, 25, 1615–1634, 1991.

Held, A. and Klemm, O.: Direct measurement of turbulent particle exchange with a twin CPC eddy covariance system, *Atmos. Environ.*, 40, S92–S102, 2006.

Hicks, B. B., Baldocchi, D. D., Meyers, T. P., Hosker, R. P., and Matt, D. R.: A preliminary multiple resistance routine for deriving dry deposition velocities from measured quantities, *Water Air Soil Pollut.*, 36, 311–330, 1987.

Hirsch, R. M. and Gilroy, E. J.: Methods of fitting a straight-line to data – examples in water-resources, *Water Resour. Bull.*, 20, 705–711, 1984.

Hogstrom, U.: Analysis of turbulence structure in the surface-layer with a modified similarity formulation for near neutral conditions, *J. Atmos. Sci.*, 47, 1949–1972, 1990.

Huebert, B. J. and Robert, C. H.: The dry deposition of nitric-acid to grass, *J. Geophys. Res.-Atmos.*, 90, 2085–2090, 1985.

Huey, L. G.: Measurement of trace atmospheric species by chemical ionization mass spectrometry: Speciation of reactive nitrogen and future directions, *Mass Spectrom. Rev.*, 26, 166–184, 2007.

Jaeggi, M., Ammann, C., Neftel, A., and Fuhrer, J.: Environmental control of profiles of ozone

- concentration in a grassland canopy, *Atmos. Environ.*, 40, 5496–5507, 2006.
- Jensen, N. O. and Hummelshoj, P.: Derivation of canopy resistance for water-vapor fluxes over a spruce forest, using a new technique for the viscous sublayer resistance, *Agr. Forest Meteorol.*, 73, 339–352, 1995.
- 5 Jensen, N. O. and Hummelshoj, P.: Derivation of canopy resistance for water vapor fluxes over a spruce forest, using a new technique for the viscous sublayer resistance (vol 73, 339 p., 1995), *Agr. Forest Meteorol.*, 85, 289–289, 1997.
- Kaiser, H. and Specker, H.: Bewertung und Vergleich von Analyseverfahren, *Z. analyt. Chem.*, 149, 46–66, 1956.
- 10 Kleijn, D., Kohler, F., Baldi, A., Batary, P., Concepcion, E. D., Clough, Y., Diaz, M., Gabriel, D., Holzschuh, A., Knop, E., Kovacs, A., Marshall, E. J. P., Tschardtke, T., and Verhulst, J.: On the relationship between farmland biodiversity and land-use intensity in Europe, *Proc. R. Soc. B Biol. Sci.*, 276, 903–909, 2009.
- Klemm, O., Held, A., Forkel, R., Gasche, R., Kanter, H. J., Rappengluck, B., Steinbrecher, R., Muller, K., Plewka, A., Cojocariu, C., Kreuzwieser, J., Valverde-Canossa, J., Schuster, G., Moortgat, G. K., Graus, M., and Hansel, A.: Experiments on forest/atmosphere exchange: climatology and fluxes during two summer campaigns in NE Bavaria, *Atmos. Environ.*, 40, S3–S20, 2006.
- 15 Kruit, R. J. W., van Pul, W. A. J., Otjes, R. P., Hofschreuder, P., Jacobs, A. F. G., and Holtslag, A. A. M.: Ammonia fluxes and derived canopy compensation points over non-fertilized agricultural grassland in The Netherlands using the new gradient ammonia – high accuracy – monitor (GRAHAM), *Atmos. Environ.*, 41, 1275–1287, 2007.
- 20 Krupa, S. V.: Effects of atmospheric ammonia ( $\text{NH}_3$ ) on terrestrial vegetation: a review, *Environ. Pollut.*, 124, 179–221, 2003.
- 25 Meyers, T. P., Huebert, B. J., and Hicks, B. B.:  $\text{HNO}_3$  deposition to a deciduous forest, *Bound.-Lay. Meteorol.*, 49, 395–410, 1989.
- Milford, C., Hargreaves, K. J., Sutton, M. A., Loubet, B., and Cellier, P.: Fluxes of  $\text{NH}_3$  and  $\text{CO}_2$  over upland moorland in the vicinity of agricultural land, *J. Geophys. Res.-Atmos.*, 106, 24169–24181, 2001.
- 30 Miller, J. C. and Miller, J. N.: *Statistics for analytical chemistry*, 2nd edition ed., Ellis Horwood series in analytical chemistry, edited by: Chalmers, R. A., and Masson, M., W. Sussex, 1988.
- Mozurkewich, M.: The dissociation constant of ammonium nitrate and its dependence on temperature, relative humidity and particle size, *Atmos. Environ. A Gen. Top.*, 27, 261–270,

---

## An analysis of precision requirements and flux errors

V. Wolff et al.

---

Title Page

Abstract

Introduction

Conclusions

References

Tables

Figures

⏪

⏩

◀

▶

Back

Close

Full Screen / Esc

Printer-friendly Version

Interactive Discussion

1993.

Mueller, H., Kramm, G., Meixner, F., Dollard, G. J., Fowler, D., and Possanzini, M.: Determination of nitric acid dry deposition by modified Bowen ratio and aerodynamic profile techniques, *Tellus Ser. B Chem. Phys. Meteorol.*, 45, 346–367, 1993.

5 Neftel, A., Flechard, C., Ammann, C., Conen, F., Emmenegger, L., and Zeyer, K.: Experimental assessment of N<sub>2</sub>O background fluxes in grassland systems, *Tellus Ser. B Chem. Phys. Meteorol.*, 59, 470–482, 2007.

Neftel, A., Spirig, C., and Ammann, C.: Application and test of a simple tool for operational footprint evaluations, *Environ. Pollut.*, 152, 644–652, 2008.

10 Nemitz, E., Sutton, M. A., Wyers, G. P., Otjes, R. P., Schjoerring, J. K., Gallagher, M. W., Parrington, J., Fowler, D., and Choulaton, T. W.: Surface/atmosphere exchange and chemical interaction of gases and aerosols over oilseed rape, *Agr. Forest Meteorol.*, 105, 427–445, 2000.

15 Nemitz, E. and Sutton, M. A.: Gas-particle interactions above a Dutch heathland: III. Modelling the influence of the NH<sub>3</sub>-HNO<sub>3</sub>-NH<sub>4</sub>NO<sub>3</sub> equilibrium on size-segregated particle fluxes, *Atmos. Chem. Phys.*, 4, 1025–1045, 2004, <http://www.atmos-chem-phys.net/4/1025/2004/>.

20 Nemitz, E., Sutton, M. A., Wyers, G. P., and Jongejan, P. A. C.: Gas-particle interactions above a Dutch heathland: I. Surface exchange fluxes of NH<sub>3</sub>, SO<sub>2</sub>, HNO<sub>3</sub> and HCl, *Atmos. Chem. Phys.*, 4, 989–1005, 2004a, <http://www.atmos-chem-phys.net/4/989/2004/>.

25 Nemitz, E., Sutton, M. A., Wyers, G. P., Otjes, R. P., Mennen, M. G., van Putten, E. M., and Gallagher, M. W.: Gas-particle interactions above a Dutch heathland: II. Concentrations and surface exchange fluxes of atmospheric particles, *Atmos. Chem. Phys.*, 4, 1007–1024, 2004b, <http://www.atmos-chem-phys.net/4/1007/2004/>.

30 Nemitz, E., Jimenez, J. L., Huffman, J. A., Ulbrich, I. M., Canagaratna, M. R., Worsnop, D. R., and Guenther, A. B.: An eddy-covariance system for the measurement of surface/atmosphere exchange fluxes of submicron aerosol chemical species – First application above an urban area, *Aerosol Sci. Technol.*, 42, 636–657, 2008.

Norman, M., Spirig, C., Wolff, V., Trebs, I., Flechard, C., Wisthaler, A., Schnitzhofer, R., Hansel, A., and Neftel, A.: Intercomparison of ammonia measurement techniques at an intensively managed grassland site (Oensingen, Switzerland), *Atmos. Chem. Phys.*, 9, 2635–

**An analysis of  
precision  
requirements and  
flux errors**

V. Wolff et al.

Title Page

Abstract

Introduction

Conclusions

References

Tables

Figures

⏪

⏩

◀

▶

Back

Close

Full Screen / Esc

Printer-friendly Version

Interactive Discussion

2645, 2009,

<http://www.atmos-chem-phys.net/9/2635/2009/>.

Phillips, S. B., Arya, S. P., and Aneja, V. P.: Ammonia flux and dry deposition velocity from near-surface concentration gradient measurements over a grass surface in North Carolina, *Atmos. Environ.*, **38**, 3469–3480, 2004.

Plassmann, K., Edwards-Jones, G., and Jones, M. L. M.: The effects of low levels of nitrogen deposition and grazing on dune grassland, *Sci. Total Environ.*, **407**, 1391–1404, 2009.

Pryor, S. C., Barthelmie, R. J., Jensen, B., Jensen, N. O., and Sorensen, L. L.: HNO<sub>3</sub> fluxes to a deciduous forest derived using gradient and REA methods, *Atmos. Environ.*, **36**, 5993–5999, 2002.

Ratray, G. and Sievering, H.: Dry deposition of ammonia, nitric acid, ammonium, and nitrate to alpine tundra at Niwot Ridge, Colorado, *Atmos. Environ.*, **35**, 1105–1109, 2001.

Rebmann, C., Gockede, M., Foken, T., Aubinet, M., Aurela, M., Berbigier, P., Bernhofer, C., Buchmann, N., Carrara, A., Cescatti, A., Ceulemans, R., Clement, R., Elbers, J. A., Granier, A., Grunwald, T., Guyon, D., Havrankova, K., Heinesch, B., Knohl, A., Laurila, T., Longdoz, B., Marcolla, B., Markkanen, T., Miglietta, F., Moncrieff, J., Montagnani, L., Moors, E., Nardino, M., Ourcival, J. M., Rambal, S., Rannik, U., Rotenberg, E., Sedlak, P., Unterhuber, G., Vesala, T., and Yakir, D.: Quality analysis applied on eddy covariance measurements at complex forest sites using footprint modelling, *Theor. Appl. Climatol.*, **80**, 121–141, 2005.

Remke, E., Brouwer, E., Kooijman, A., Blindow, I., Esselink, H., and Roelofs, J. G. M.: Even low to medium nitrogen deposition impacts vegetation of dry, coastal dunes around the Baltic Sea, *Environ. Pollut.*, **157**, 792–800, 2009.

Richardson, A. D., Hollinger, D. Y., Burba, G. G., Davis, K. J., Flanagan, L. B., Katul, G. G., Munger, J. W., Ricciuto, D. M., Stoy, P. C., Suyker, A. E., Verma, S. B., and Wofsy, S. C.: A multi-site analysis of random error in tower-based measurements of carbon and energy fluxes, *Agricultural and Forest Meteorology*, **136**, 1–18, 2006.

Schmidt, A. and Klemm, O.: Direct determination of highly size-resolved turbulent particle fluxes with the disjunct eddy covariance method and a 12-stage electrical low pressure impactor, *Atmos. Chem. Phys.*, **8**, 7405–7417, 2008,

<http://www.atmos-chem-phys.net/8/7405/2008/>.

Seinfeld, J. H. and Pandis, S. N.: *Atmospheric Chemistry and Physics: From Air Pollution to Climate Change*, Wiley, New York, 2006.

**AMTD**

2, 2423–2482, 2009

## An analysis of precision requirements and flux errors

V. Wolff et al.

Title Page

Abstract

Introduction

Conclusions

References

Tables

Figures

⏪

⏩

◀

▶

Back

Close

Full Screen / Esc

Printer-friendly Version

Interactive Discussion

**An analysis of  
precision  
requirements and  
flux errors**

V. Wolff et al.

Title Page

Abstract

Introduction

Conclusions

References

Tables

Figures

◀

▶

◀

▶

Back

Close

Full Screen / Esc

Printer-friendly Version

Interactive Discussion

- Sievering, H., Enders, G., Kins, L., Kramm, G., Ruoss, K., Roider, G., Zelger, M., Anderson, L., and Dlugi, R.: Nitric-acid, particulate nitrate and ammonium profiles at the Bayerischer Wald – Evidence for large deposition rates of total nitrate, *Atmos. Environ.*, 28, 311–315, 1994.
- 5 Sievering, H., Kelly, T., McConville, G., Seibold, C., and Turnipseed, A.: Nitric acid dry deposition to conifer forests: Niwot Ridge spruce-fir-pine study, *Atmos. Environ.*, 35, 3851–3859, 2001.
- Simpson, I. J., Thurtell, G. W., Neumann, H. H., Den Hartog, G., and Edwards, G. C.: The validity of similarity theory in the roughness sublayer above forests, *Bound.-Lay. Meteorol.*, 87, 69–99, 1998.
- 10 Spindler, G., Teichmann, U., and Sutton, M. A.: Ammonia dry deposition over grassland – micrometeorological flux-gradient measurements and bidirectional flux calculations using an inferential model, *Q. J. Roy. Meteorol. Soc.*, 127, 795–814, 2001.
- Staudt, K. and Foken, T.: Documentation of reference data for the experimental areas of the Bayreuth Center for Ecology and Environmental Research (BayCEER) at the Waldstein site, Dep. Micromet., University of Bayreuth, 2007.
- 15 Stelson, A. W. and Seinfeld, J. H.: Relative-humidity and temperature-dependence of the ammonium-nitrate dissociation-constant, *Atmos. Environ.*, 16, 983–992, 1982.
- Sutton, M. A., Nemitz, E., Fowler, D., Wyers, G. P., Otjes, R. P., Schjoerring, J. K., Husted, S., Nielsen, K. H., San Jose, R., Moreno, J., Gallagher, M. W., and Gut, A.: Fluxes of ammonia over oilseed rape – Overview of the EXAMINE experiment, *Agr. Forest Meteorol.*, 105, 327–349, 2000a.
- 20 Sutton, M. A., Nemitz, E., Milford, C., Fowler, D., Moreno, J., San Jose, R., Wyers, G. P., Otjes, R. P., Harrison, R., Husted, S., and Schjoerring, J. K.: Micrometeorological measurements of net ammonia fluxes over oilseed rape during two vegetation periods, *Agr. Forest Meteorol.*, 105, 351–369, 2000b.
- 25 Sutton, M. A., Nemitz, E., Erisman, J. W., Beier, C., Bahl, K. B., Cellier, P., de Vries, W., Cotrufo, F., Skiba, U., Di Marco, C., Jones, S., Laville, P., Soussana, J. F., Loubet, B., Twigg, M., Famulari, D., Whitehead, J., Gallagher, M. W., Neftel, A., Flechard, C. R., Herrmann, B., Calanca, P. L., Schjoerring, J. K., Daemmgen, U., Horvath, L., Tang, Y. S., Emmett, B. A., Tietema, A., Penuelas, J., Kesik, M., Brueggemann, N., Pilegaard, K., Vesala, T., Campbell, C. L., Olesen, J. E., Dragosits, U., Theobald, M. R., Levy, P., Mobbs, D. C., Milne, R., Viovy, N., Vuichard, N., Smith, J. U., Smith, P., Bergamaschi, P., Fowler, D., and Reis, S.: Challenges in quantifying biosphere-atmosphere exchange of nitrogen species, *Environmental Pollution*,
- 30

150, 125–139, 2007.

Thom, A. S., Stewart, J. B., Oliver, H. R., and Gash, J. H. C.: Comparison of aerodynamic and energy budget estimates of fluxes over a pine forest, *Q. J. Roy. Meteorol. Soc.*, 101, 93–105, 1975.

5 Thomas, C. and Foken, T.: Flux contribution of coherent structures and its implications for the exchange of energy and matter in a tall spruce canopy, *Bound.-Lay. Meteorol.*, 123, 317–337, 2007.

Thomas, R. M., Trebs, I., Otjes, R., Jongejan, P. A. C., Brink, H. T., Phillips, G., Kortner, M., Meixner, F. X., and Nemitz, E.: An automated analyzer to measure surface-atmosphere  
10 exchange fluxes of water soluble inorganic aerosol compounds and reactive trace gases, *Environ. Sci. Technol.*, 43, 1412–1418, doi:10.1021/es8019403, 2009.

Trebs, I., Meixner, F. X., Slanina, J., Otjes, R., Jongejan, P., and Andreae, M. O.: Real-time measurements of ammonia, acidic trace gases and water-soluble inorganic aerosol species at a rural site in the Amazon Basin, *Atmos. Chem. Phys.*, 4, 967–987, 2004,  
15 <http://www.atmos-chem-phys.net/4/967/2004/>.

Van Oss, R., Duyzer, J., and Wyers, P.: The influence of gas-to-particle conversion on measurements of ammonia exchange over forest, *Atmos. Environ.*, 32, 465–471, 1998.

Vickers, D. and Mahrt, L.: Quality control and flux sampling problems for tower and aircraft data, *J. Atmos. Ocean. Technol.*, 14, 512–526, 1997.

20 Wesely, M. L. and Hicks, B. B.: A review of the current status of knowledge on dry deposition, *Atmos. Environ.*, 34, 2261–2282, 2000.

Wichura, B., Ruppert, J., Delany, A. C., Buchmann, N., and Foken, T.: Structure of carbon dioxide exchange processes above a spruce forest, in: *Biogeochemistry of Forested Catchments in a Changing Environment: an German Case Study*, Ecological Studies: Analysis and Synthesis, Springer-Verlag, Berlin, 161–176, 2004.

25 Wyers, G. P., Vermeulen, A. T., and Slanina, J.: Measurement of dry deposition of ammonia on a forest, *Environ. Pollut.*, 75, 25–28, 1992.

Wyers, G. P., Otjes, R. P., and Slanina, J.: A continuous-flow denuder for the measurement of ambient concentrations and surface-exchange fluxes of ammonia, *Atmos. Environ. A Gen. Top.*, 27, 2085–2090, 1993.

30 Wyers, G. P. and Duyzer, J. H.: Micrometeorological measurement of the dry deposition flux of sulphate and nitrate aerosols to coniferous forest, *Atmos. Environ.*, 31, 333–343, 1997.

Wyers, G. P. and Erisman, J. W.: Ammonia exchange over coniferous forest, *Atmos. Environ.*,

## An analysis of precision requirements and flux errors

V. Wolff et al.

Title Page

Abstract

Introduction

Conclusions

References

Tables

Figures

◀

▶

◀

▶

Back

Close

Full Screen / Esc

Printer-friendly Version

Interactive Discussion

32, 441–451, 1998.

Zheng, J., Zhang, R., Fortner, E. C., Volkamer, R. M., Molina, L., Aiken, A. C., Jimenez, J. L., Gaeggeler, K., Dommen, J., Dusanter, S., Stevens, P. S., and Tie, X.: Measurements of  $\text{HNO}_3$  and  $\text{N}_2\text{O}_5$  using ion drift-chemical ionization mass spectrometry during the MILAGRO/MCMA-2006 campaign, *Atmos. Chem. Phys.*, 8, 6823–6838, 2008, <http://www.atmos-chem-phys.net/8/6823/2008/>.

**AMTD**

2, 2423–2482, 2009

---

**An analysis of  
precision  
requirements and  
flux errors**

V. Wolff et al.

---

Title Page

Abstract

Introduction

Conclusions

References

Tables

Figures

◀

▶

◀

▶

Back

Close

Full Screen / Esc

Printer-friendly Version

Interactive Discussion

**An analysis of  
precision  
requirements and  
flux errors**

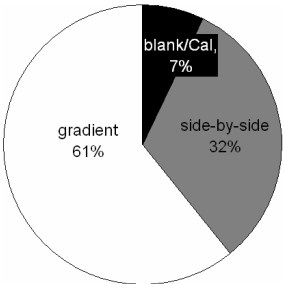
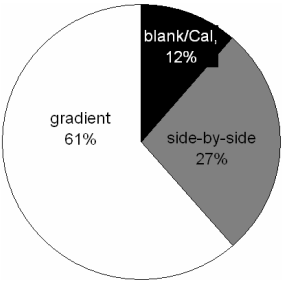
V. Wolff et al.

**Table 1.** Limits of detection ( $3\sigma$ -definition) for the gas/particle concentrations determined under field conditions at the two campaign sites.

	NEU		EGER	
	$\mu\text{g m}^{-3}$ in air		$\mu\text{g m}^{-3}$ in air	
$\text{NH}_3/\text{NH}_4^+$	0.055	0.074	0.021	0.022
$\text{HNO}_3/\text{NO}_3^-$	0.094	0.093	0.132	0.130

[Title Page](#)[Abstract](#)[Introduction](#)[Conclusions](#)[References](#)[Tables](#)[Figures](#)[I◀](#)[▶I](#)[◀](#)[▶](#)[Back](#)[Close](#)[Full Screen / Esc](#)[Printer-friendly Version](#)[Interactive Discussion](#)

**Table 2.** Overview of the data availability for the two experiments (NEU, grassland, Switzerland, 2006, and EGER, forest, Germany, 2007). SB1 and SB2: sample box one and sample box two. For the concentration differences,  $\Delta C$ , only values with both concentration values >LOD were used.

NEU		Side-by-side			Gradient			
		Tot No.	<LOD	No. of $\Delta C$	Tot No.	<LOD	No. of $\Delta C$	
	$\text{NH}_3$	SB1	188	1%	146	612	0%	490
		SB2	202	1%		515	0%	
	$\text{NH}_4^+$	SB1	106	35%	27	550	11%	251
		SB2	90	53%		365	24%	
	$\text{HNO}_3$	SB1	145	19%	91	478	18%	271
		SB2	194	10%		345	7%	
	$\text{NO}_3^-$	SB1	108	2%	62	535	0%	316
		SB2	174	3%		340	2%	
EGER		Side-by-side			Gradient			
		Tot No.	< LOD	No. of $\Delta C$	Tot No.	<LOD	No. of $\Delta C$	
	$\text{NH}_3$	SB1	20	4%	148	528	1%	482
		SB2	184	9%		495	0%	
	$\text{NH}_4^+$	SB1	230	1%	198	501	1%	451
		SB2	219	1%		495	2%	
	$\text{HNO}_3$	SB1	216	8%	176	449	31%	284
		SB2	219	19%		433	31%	
	$\text{NO}_3^-$	SB1	215	2%	203	486	6%	409
		SB2	232	3%		454	10%	

An analysis of precision requirements and flux errors

V. Wolff et al.

Title Page

Abstract Introduction

Conclusions References

Tables Figures

⏪ ⏩

◀ ▶

Back Close

Full Screen / Esc

Printer-friendly Version

Interactive Discussion



## An analysis of precision requirements and flux errors

V. Wolff et al.

**Table 3.** Laplace and Gaussian standard deviations,  $\text{std}_{\Delta C}$  of the residuals of the concentration difference obtained during the side-by-side measurements after correcting the data for systematic deviations using the orthogonal fit for NEU and EGER.

	NEU		EGER	
	Laplace std $\mu\text{g m}^{-3}$	Gauss std $\mu\text{g m}^{-3}$	Laplace std $\mu\text{g m}^{-3}$	Gauss std $\mu\text{g m}^{-3}$
$\text{NH}_3$	0.400	0.404	0.091	0.106
$\text{NH}_4^+$	0.143	0.132	0.132	0.134
$\text{HNO}_3$	0.095	0.093	0.131	0.160
$\text{NO}_3^-$	0.117	0.114	0.484	0.441

Title Page

Abstract

Introduction

Conclusions

References

Tables

Figures

⏪

⏩

◀

▶

Back

Close

Full Screen / Esc

Printer-friendly Version

Interactive Discussion

## An analysis of precision requirements and flux errors

V. Wolff et al.

**Table 4.** Errors of the concentration difference, relative to the ambient concentration,  $\sigma_{\Delta C}/C$ , determined for NEU and EGER. For particulate  $\text{NH}_4^+$  during NEU and particulate  $\text{NO}_3^-$  during EGER only absolute values independent of  $C$  could be determined (see text and Table 3).

	NEU	EGER
	$\sigma_{\Delta C}/C_{\text{ambient}}, \%$	$\sigma_{\Delta C}/C_{\text{ambient}}, \%$
$\text{NH}_3$	5.99	8.09
$\text{NH}_4^+$	–	6.61
$\text{HNO}_3$	6.13	10.39
$\text{NO}_3^-$	5.48	–

Title Page

Abstract

Introduction

Conclusions

References

Tables

Figures

◀

▶

◀

▶

Back

Close

Full Screen / Esc

Printer-friendly Version

Interactive Discussion

## An analysis of precision requirements and flux errors

V. Wolff et al.

**Table 5.** Percentage of significant  $\Delta C$  (values larger than  $\sigma_{\Delta C}$ ) during gradient measurements for NEU and EGER.

	NEU Number of significant $\Delta C$ (% of total)	EGER Number of significant $\Delta C$ (% of total)
$\text{NH}_3$	263 (54%)	245 (51%)
$\text{NH}_4^+$	60 (24%)	221 (49%)
$\text{HNO}_3$	119 (44%)	128 (45%)
$\text{NO}_3^-$	123 (39%)	43 (11%)

Title Page

Abstract

Introduction

Conclusions

References

Tables

Figures

⏪

⏩

◀

▶

Back

Close

Full Screen / Esc

Printer-friendly Version

Interactive Discussion

**Table 6.** List of studies that have performed aerodynamic gradient measurements of  $\text{NH}_3$ ,  $\text{HNO}_3$ , particulate  $\text{NH}_4^+/\text{NO}_3^-$ . Indicated are the measured species, whether or not the method was continuous or semi-continuous, and whether a precision (error) estimate was used to derive and discuss exchange fluxes.

		$\text{NH}_3$	$\text{HNO}_3$	$\text{NH}_4^+$	$\text{NO}_3^-$	Continuous/ semi-continuous	Flux error estimate
(1)	(Huebert and Robert, 1985)	<input type="checkbox"/>	<input checked="" type="checkbox"/>	<input type="checkbox"/>	<input checked="" type="checkbox"/>	<input type="checkbox"/>	<input checked="" type="checkbox"/>
(2)	(Erisman et al., 1988)	<input checked="" type="checkbox"/>	<input checked="" type="checkbox"/>	<input checked="" type="checkbox"/>	<input checked="" type="checkbox"/>	<input type="checkbox"/>	<input type="checkbox"/>
(3)	(Duyzer et al., 1992)	<input checked="" type="checkbox"/>	<input type="checkbox"/>	<input type="checkbox"/>	<input type="checkbox"/>	<input type="checkbox"/>	<input type="checkbox"/>
(4)	(Wyers et al., 1992)	<input checked="" type="checkbox"/>	<input type="checkbox"/>	<input type="checkbox"/>	<input type="checkbox"/>	<input checked="" type="checkbox"/>	<input type="checkbox"/>
(5)	(Andersen et al., 1993)	<input checked="" type="checkbox"/>	<input checked="" type="checkbox"/>	<input checked="" type="checkbox"/>	<input checked="" type="checkbox"/>	<input type="checkbox"/>	<input type="checkbox"/>
(6)	(Erisman and Wyers, 1993)	<input checked="" type="checkbox"/>	<input type="checkbox"/>	<input type="checkbox"/>	<input type="checkbox"/>	<input type="checkbox"/>	<input checked="" type="checkbox"/>
(7)	(Duyzer, 1994)	<input checked="" type="checkbox"/>	<input type="checkbox"/>	<input type="checkbox"/>	<input type="checkbox"/>	<input type="checkbox"/>	<input checked="" type="checkbox"/>
(8)	(Sievering et al., 1994)	<input checked="" type="checkbox"/>	<input checked="" type="checkbox"/>	<input checked="" type="checkbox"/>	<input checked="" type="checkbox"/>	<input type="checkbox"/>	<input type="checkbox"/>
(9)	(Andersen and Hovmand, 1995)	<input checked="" type="checkbox"/>	<input checked="" type="checkbox"/>	<input type="checkbox"/>	<input type="checkbox"/>	<input type="checkbox"/>	<input type="checkbox"/>
(10)	(Wyers and Duyzer, 1997)	<input type="checkbox"/>	<input type="checkbox"/>	<input checked="" type="checkbox"/>	<input checked="" type="checkbox"/>	<input checked="" type="checkbox"/>	<input type="checkbox"/>
(11)	(Flechar and Fowler, 1998)	<input checked="" type="checkbox"/>	<input type="checkbox"/>	<input type="checkbox"/>	<input type="checkbox"/>	<input checked="" type="checkbox"/>	<input checked="" type="checkbox"/>
(12)	(Van Oss et al., 1998)	<input checked="" type="checkbox"/>	<input checked="" type="checkbox"/>	<input checked="" type="checkbox"/>	<input checked="" type="checkbox"/>	<input type="checkbox"/>	<input type="checkbox"/>
(13)	(Wyers and Erisman, 1998)	<input checked="" type="checkbox"/>	<input type="checkbox"/>	<input type="checkbox"/>	<input type="checkbox"/>	<input checked="" type="checkbox"/>	<input type="checkbox"/>
(14)	(Andersen et al., 1999)	<input checked="" type="checkbox"/>	<input type="checkbox"/>	<input type="checkbox"/>	<input type="checkbox"/>	<input type="checkbox"/>	<input type="checkbox"/>
(15)	(Nemitz et al., 2000)	<input checked="" type="checkbox"/>	<input type="checkbox"/>				
(16)	(Sutton et al., 2000b)	<input checked="" type="checkbox"/>	<input type="checkbox"/>	<input type="checkbox"/>	<input type="checkbox"/>	<input checked="" type="checkbox"/>	<input type="checkbox"/>
(17)	(Milford et al., 2001)	<input checked="" type="checkbox"/>	<input type="checkbox"/>	<input type="checkbox"/>	<input type="checkbox"/>	<input checked="" type="checkbox"/>	<input type="checkbox"/>
(18)	(Ratray and Sievering, 2001)	<input checked="" type="checkbox"/>	<input checked="" type="checkbox"/>	<input checked="" type="checkbox"/>	<input checked="" type="checkbox"/>	<input type="checkbox"/>	<input checked="" type="checkbox"/>
(19)	(Sievering et al., 2001)	<input type="checkbox"/>	<input checked="" type="checkbox"/>	<input checked="" type="checkbox"/>	<input checked="" type="checkbox"/>	<input type="checkbox"/>	<input type="checkbox"/>
(20)	(Spindler et al., 2001)	<input checked="" type="checkbox"/>	<input type="checkbox"/>	<input type="checkbox"/>	<input type="checkbox"/>	<input checked="" type="checkbox"/>	<input type="checkbox"/>
(21)	(Pryor et al., 2002)	<input type="checkbox"/>	<input type="checkbox"/>	<input type="checkbox"/>	<input type="checkbox"/>	<input checked="" type="checkbox"/>	<input type="checkbox"/>
(22)	(Nemitz et al., 2004a)	<input checked="" type="checkbox"/>	<input type="checkbox"/>				
(23)	(Nemitz et al., 2004b)	<input checked="" type="checkbox"/>	<input type="checkbox"/>				
(24)	(Nemitz and Sutton, 2004)	<input checked="" type="checkbox"/>	<input type="checkbox"/>				
(25)	(Phillips et al., 2004)	<input checked="" type="checkbox"/>	<input type="checkbox"/>	<input type="checkbox"/>	<input type="checkbox"/>	<input checked="" type="checkbox"/>	<input type="checkbox"/>
(26)	(Kruit et al., 2007)	<input checked="" type="checkbox"/>	<input type="checkbox"/>	<input type="checkbox"/>	<input type="checkbox"/>	<input checked="" type="checkbox"/>	<input type="checkbox"/>
(27)	(Thomas et al., 2009)	<input checked="" type="checkbox"/>					

## An analysis of precision requirements and flux errors

V. Wolff et al.

Title Page

Abstract

Introduction

Conclusions

References

Tables

Figures

⏪

⏩

◀

▶

Back

Close

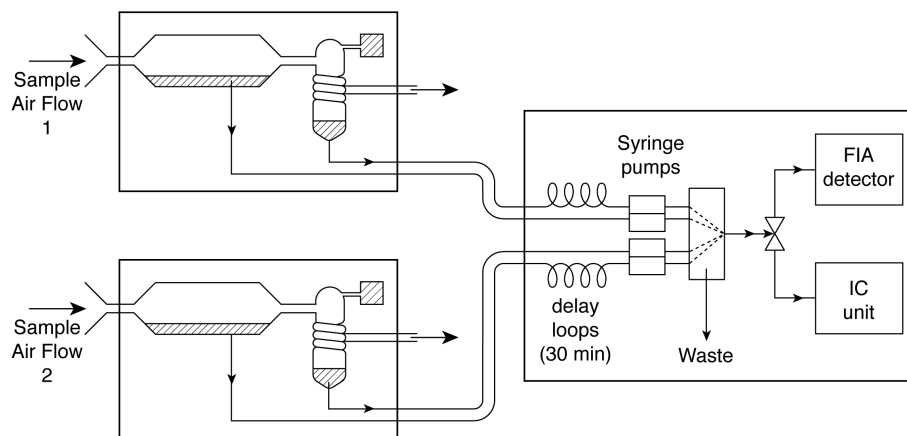
Full Screen / Esc

Printer-friendly Version

Interactive Discussion

**An analysis of  
precision  
requirements and  
flux errors**

V. Wolff et al.

**Fig. 1.** Simplified scheme of the GRAEGOR instrument.[Title Page](#)[Abstract](#)[Introduction](#)[Conclusions](#)[References](#)[Tables](#)[Figures](#)[◀](#)[▶](#)[◀](#)[▶](#)[Back](#)[Close](#)[Full Screen / Esc](#)[Printer-friendly Version](#)[Interactive Discussion](#)

## An analysis of precision requirements and flux errors

V. Wolff et al.

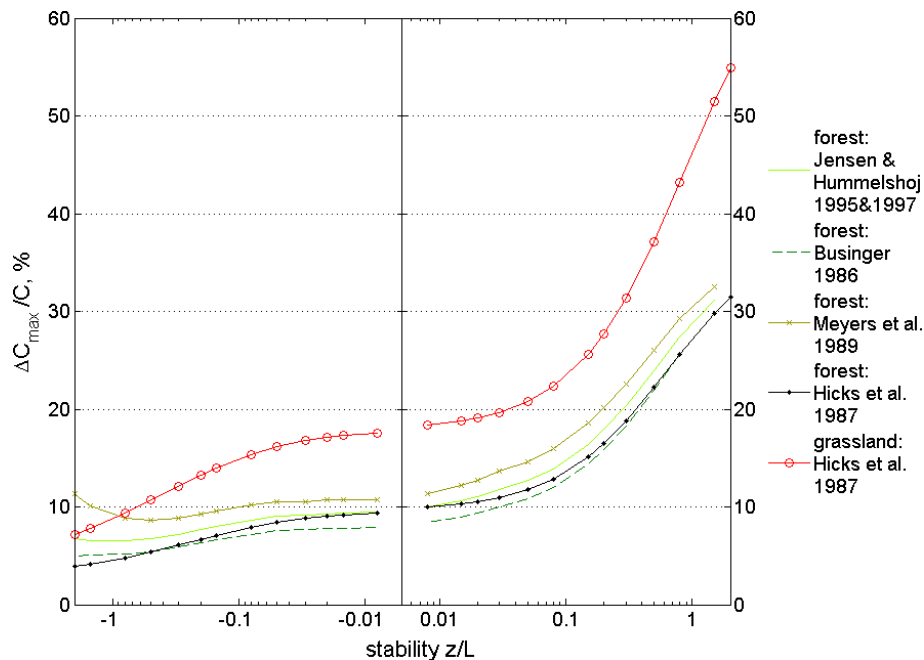


**Fig. 2.** Minimal relative precision requirements ( $\Delta C_{\max}/C$  in %) assuming a maximum  $\text{HNO}_3$  deposition flux ( $R_c=0$ ) for a grassland site (NEU) and a forest site (EGER). For the forest site different parameterizations for  $R_b$  existing in literature (Businger, 1986; Jensen and Hummelshoj, 1995; Jensen and Hummelshoj, 1997; Meyers et al., 1989) are applied. Note that in the formulation of  $R_a$  for the forest no correction was introduced for a roughness sublayer.

Title Page

Abstract

Introduction

Conclusions

References

Tables

Figures

◀

▶

◀

▶

Back

Close

Full Screen / Esc

Printer-friendly Version

Interactive Discussion

**An analysis of  
precision  
requirements and  
flux errors**

V. Wolff et al.

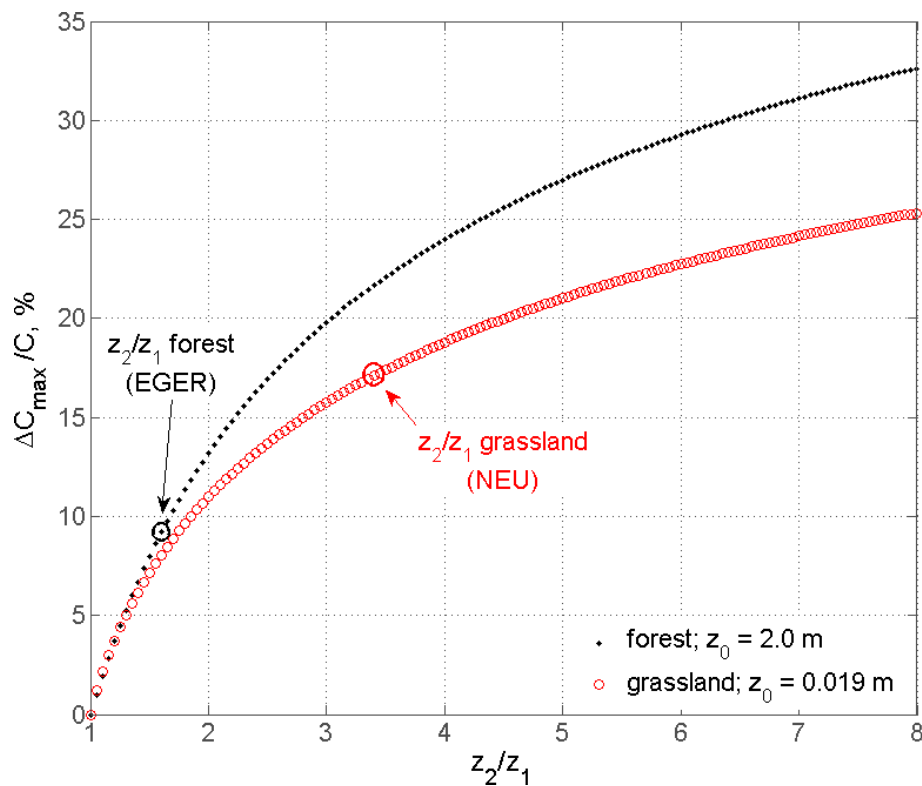


**Fig. 3.** Minimal relative precision requirements ( $\Delta C_{\max}/C$  in %) for neutral stability and a range of measurement height ratios  $z_2/z_1$  for forest and grassland. Additionally indicated are  $z_2/z_1$  values for the sites used in this study.

[Title Page](#)[Abstract](#)[Introduction](#)[Conclusions](#)[References](#)[Tables](#)[Figures](#)[◀](#)[▶](#)[◀](#)[▶](#)[Back](#)[Close](#)[Full Screen / Esc](#)[Printer-friendly Version](#)[Interactive Discussion](#)

**An analysis of  
precision  
requirements and  
flux errors**

V. Wolff et al.

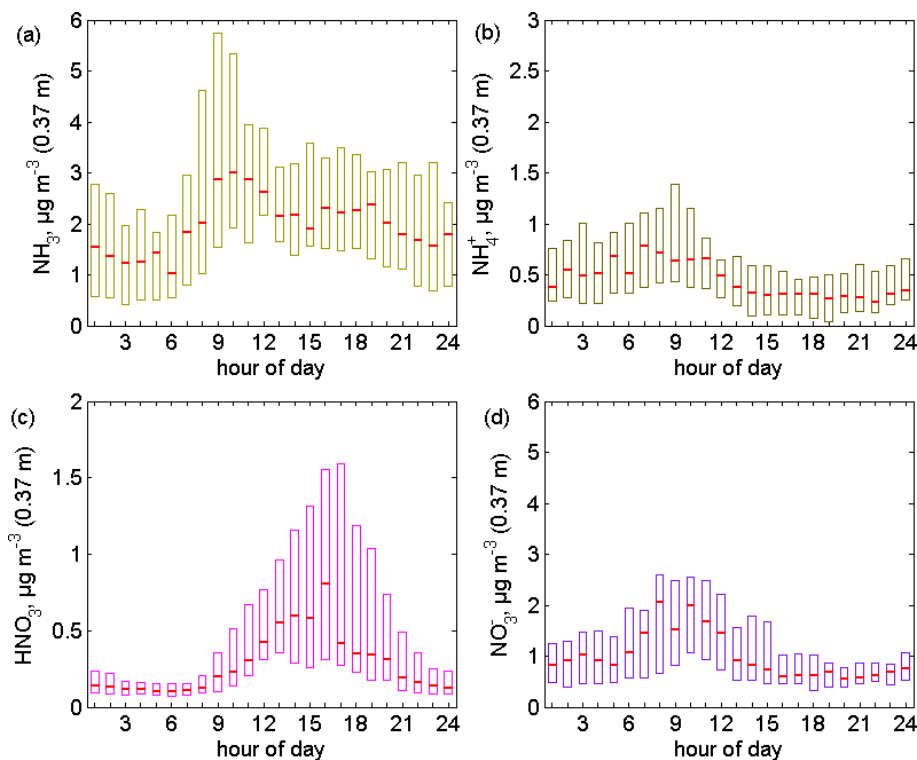


**Fig. 4.** Diel variation of (a)  $\text{NH}_3$ , (b) particulate  $\text{NH}_4^+$ , (c)  $\text{HNO}_3$ , and (d) particulate  $\text{NO}_3^-$  measured at  $z=0.37$  m (above ground). Red lines are median concentrations, boxes denote the inter-quartile range (0.25–0.75) during NEU in Oensingen (Switzerland), 2006 (managed grassland ecosystem).

[Title Page](#)[Abstract](#)[Introduction](#)[Conclusions](#)[References](#)[Tables](#)[Figures](#)[◀](#)[▶](#)[◀](#)[▶](#)[Back](#)[Close](#)[Full Screen / Esc](#)[Printer-friendly Version](#)[Interactive Discussion](#)

**An analysis of  
precision  
requirements and  
flux errors**

V. Wolff et al.

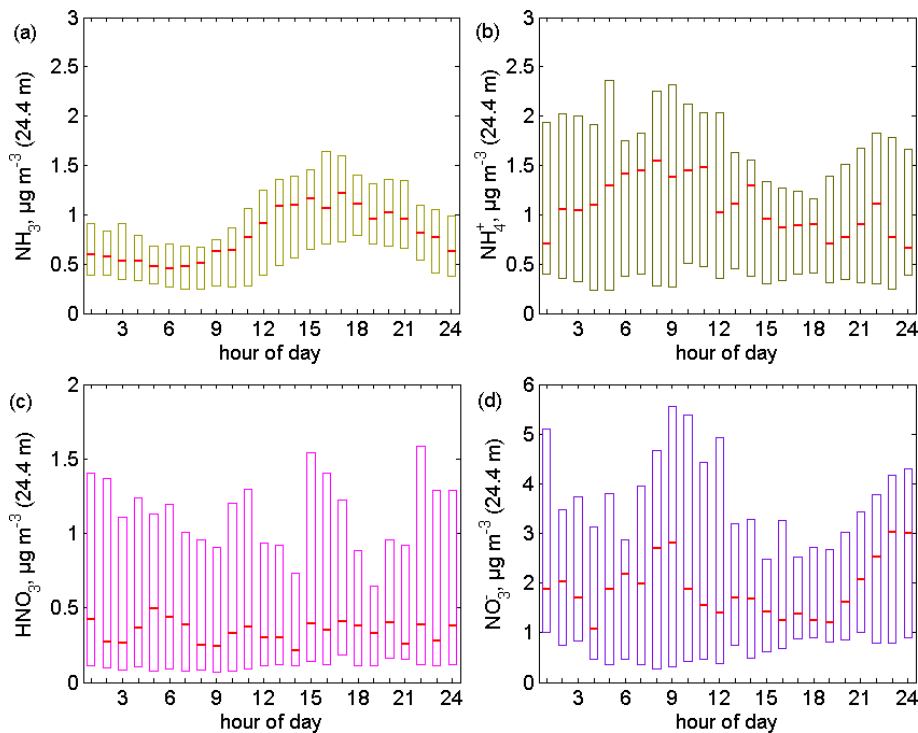


**Fig. 5.** Diel variations of (a)  $\text{NH}_3$ , (b) particulate  $\text{NH}_4^+$ , (c)  $\text{HNO}_3$ , and (d) particulate  $\text{NO}_3^-$  measured at  $z=24.4$  m (above ground). Red lines are median concentrations, boxes denote the inter-quartile range (0.25–0.75) during EGER in Waldstein (Germany), 2007 (spruce forest ecosystem).

[Title Page](#)[Abstract](#)[Introduction](#)[Conclusions](#)[References](#)[Tables](#)[Figures](#)[⏪](#)[⏩](#)[◀](#)[▶](#)[Back](#)[Close](#)[Full Screen / Esc](#)[Printer-friendly Version](#)[Interactive Discussion](#)

**An analysis of  
precision  
requirements and  
flux errors**

V. Wolff et al.

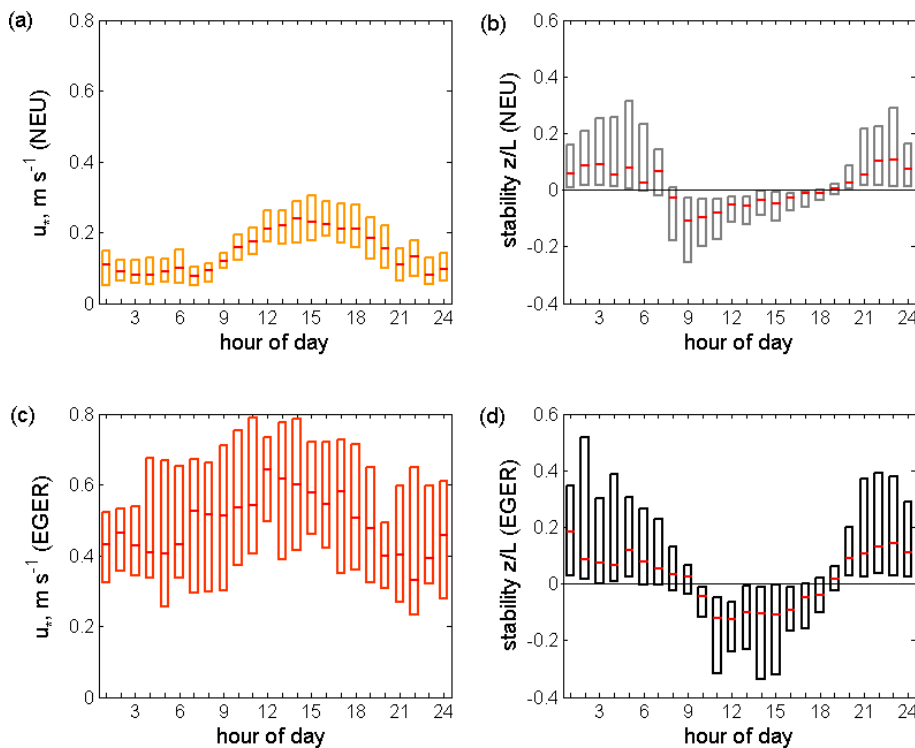


**Fig. 6.** Diel variation of friction velocity during **(a)** EGER and **(c)** NEU and of the stability ( $z/L$ ) during **(b)** EGER and **(d)** NEU. Red lines denote the median, the boxes the inter-quartile ranges (0.25–0.75).

[Title Page](#)[Abstract](#)[Introduction](#)[Conclusions](#)[References](#)[Tables](#)[Figures](#)[◀](#)[▶](#)[◀](#)[▶](#)[Back](#)[Close](#)[Full Screen / Esc](#)[Printer-friendly Version](#)[Interactive Discussion](#)

**An analysis of  
precision  
requirements and  
flux errors**

V. Wolff et al.

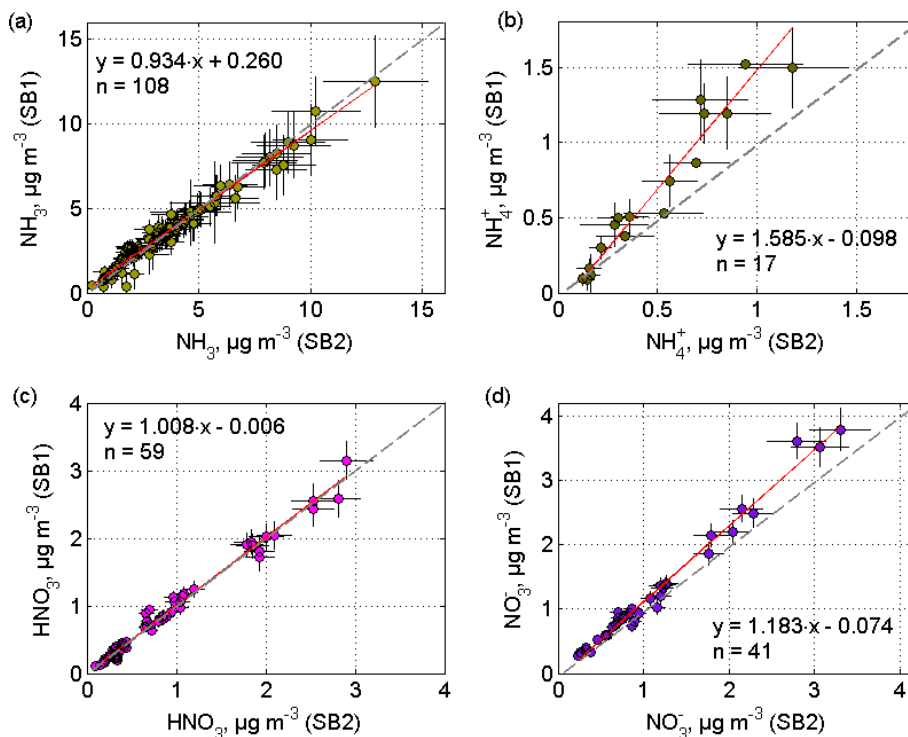


**Fig. 7.** Results from side-by-side measurements during the NEU experiment. The error bars indicate the random errors of the concentration measurements. Red lines and the given equations represent the individual orthogonal fits.  $n$  is the number of data points used for each fit. The dashed line indicates the 1:1 line. (SB1: sample box 1; height 0.37 m; SB2: sample box 2; height 1.23 m).

[Title Page](#)[Abstract](#)[Introduction](#)[Conclusions](#)[References](#)[Tables](#)[Figures](#)[◀](#)[▶](#)[◀](#)[▶](#)[Back](#)[Close](#)[Full Screen / Esc](#)[Printer-friendly Version](#)[Interactive Discussion](#)

**An analysis of  
precision  
requirements and  
flux errors**

V. Wolff et al.

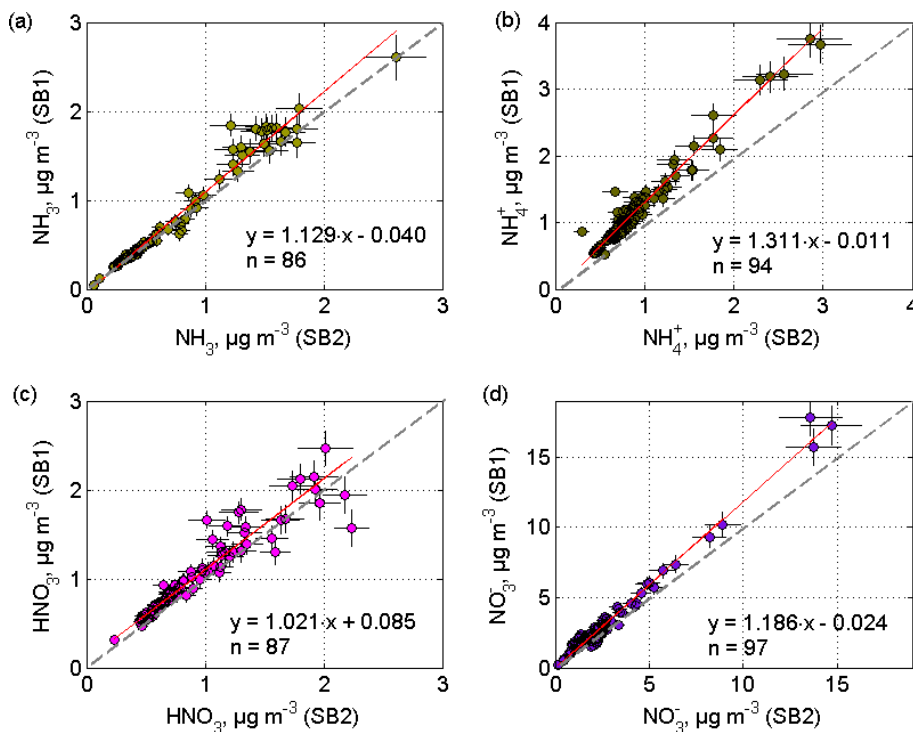


**Fig. 8.** Results from side-by-side measurements during the EGGER experiment. The error bars indicate the random errors of the concentration measurements. Red lines and the equations represent the individual orthogonal fits.  $n$  is the number of data points used for each fit. The dashed line indicates the 1:1 line. (SB1: sample box 1; height 24.4 m; SB2: sample box 2; height 30.9 m).

[Title Page](#)[Abstract](#)[Introduction](#)[Conclusions](#)[References](#)[Tables](#)[Figures](#)[◀](#)[▶](#)[◀](#)[▶](#)[Back](#)[Close](#)[Full Screen / Esc](#)[Printer-friendly Version](#)[Interactive Discussion](#)

**An analysis of  
precision  
requirements and  
flux errors**

V. Wolff et al.

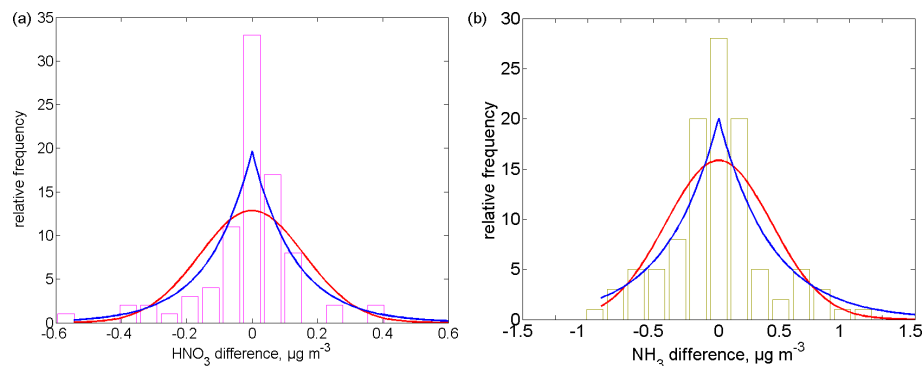


**Fig. 9.** Residuals of  $\Delta C$  for side-by-side measurements after correcting the data for systematic deviations using the orthogonal fit for **(a)** HNO<sub>3</sub> (EGER) and **(b)** NH<sub>3</sub> (NEU). The lines indicate fitted Laplace (blue) and Gaussian (red) distributions.

[Title Page](#)[Abstract](#)[Introduction](#)[Conclusions](#)[References](#)[Tables](#)[Figures](#)[⏪](#)[⏩](#)[◀](#)[▶](#)[Back](#)[Close](#)[Full Screen / Esc](#)[Printer-friendly Version](#)[Interactive Discussion](#)

**An analysis of  
precision  
requirements and  
flux errors**

V. Wolff et al.

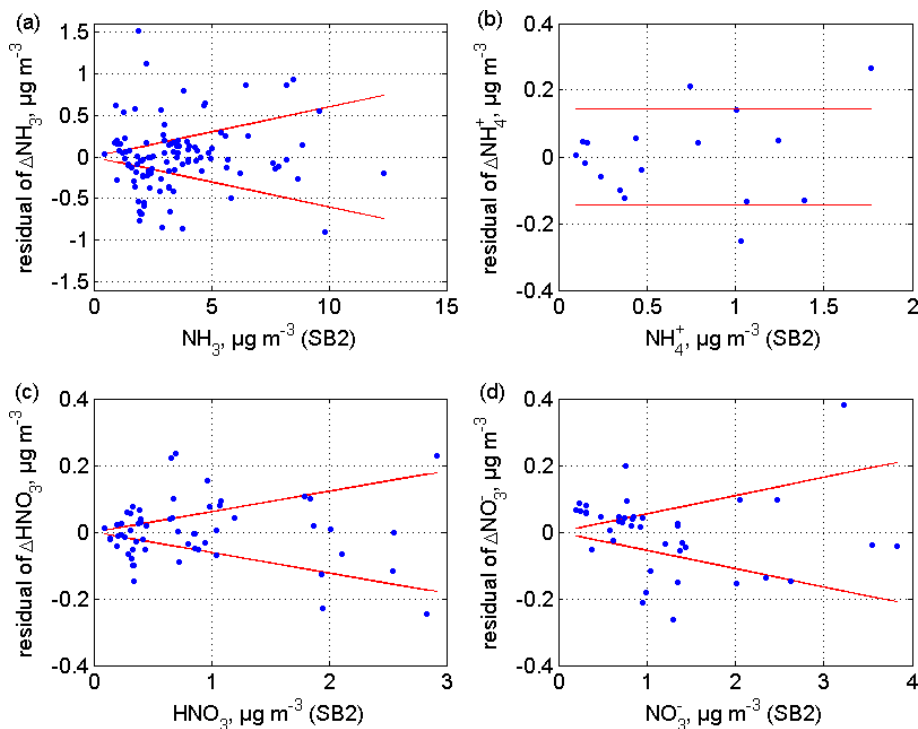


**Fig. 10.** Residuals of  $\Delta C$  during side-by-side after correcting the data for systematic deviations using the orthogonal fit (individual values: blue points) and their relation to  $C$  during NEU. The derived  $\sigma_{\Delta C}$  is shown as red line (uncertainty range around zero).

[Title Page](#)[Abstract](#)[Introduction](#)[Conclusions](#)[References](#)[Tables](#)[Figures](#)[◀](#)[▶](#)[◀](#)[▶](#)[Back](#)[Close](#)[Full Screen / Esc](#)[Printer-friendly Version](#)[Interactive Discussion](#)

**An analysis of  
precision  
requirements and  
flux errors**

V. Wolff et al.

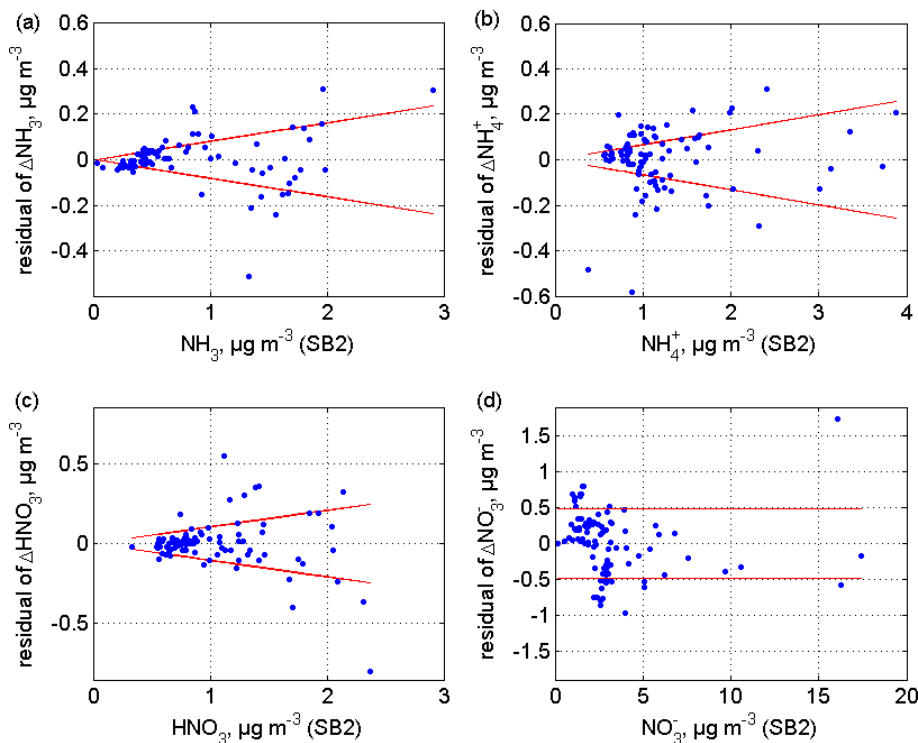


**Fig. 11.** Residuals of  $\Delta C$  during side-by-side after correcting the data for systematic deviations using the orthogonal fit (individual values: blue points) and their relation to  $C$  during EGGER. The derived  $\sigma_{\Delta C}$  is shown as red line (uncertainty range around zero).

[Title Page](#)[Abstract](#)[Introduction](#)[Conclusions](#)[References](#)[Tables](#)[Figures](#)[◀](#)[▶](#)[◀](#)[▶](#)[Back](#)[Close](#)[Full Screen / Esc](#)[Printer-friendly Version](#)[Interactive Discussion](#)

**An analysis of  
precision  
requirements and  
flux errors**

V. Wolff et al.

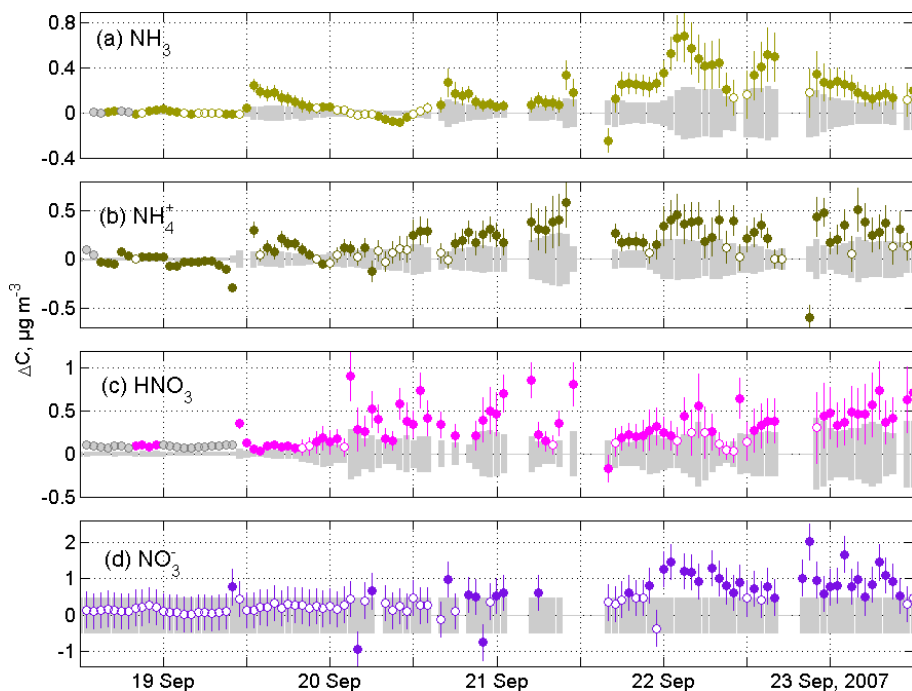


**Fig. 12.** Measured  $\Delta C$  values above the spruce forest canopy for some days during EGER. Error bars and uncertainty ranges (grey bars) for **(a)**  $\text{NH}_3$ , **(b)** particulate  $\text{NH}_4^+$ , **(c)**  $\text{HNO}_3$  and **(d)** particulate  $\text{NO}_3^-$  were determined from the residual analysis described in the text. The hollow circles are values of  $\Delta C$  that are statistically not significant different from zero, the filled circles are significant  $\Delta C$  values. Grey circles are values of  $\Delta C$  where one or both concentrations were below the LOD.

[Title Page](#)[Abstract](#)[Introduction](#)[Conclusions](#)[References](#)[Tables](#)[Figures](#)[◀](#)[▶](#)[◀](#)[▶](#)[Back](#)[Close](#)[Full Screen / Esc](#)[Printer-friendly Version](#)[Interactive Discussion](#)

**An analysis of  
precision  
requirements and  
flux errors**

V. Wolff et al.

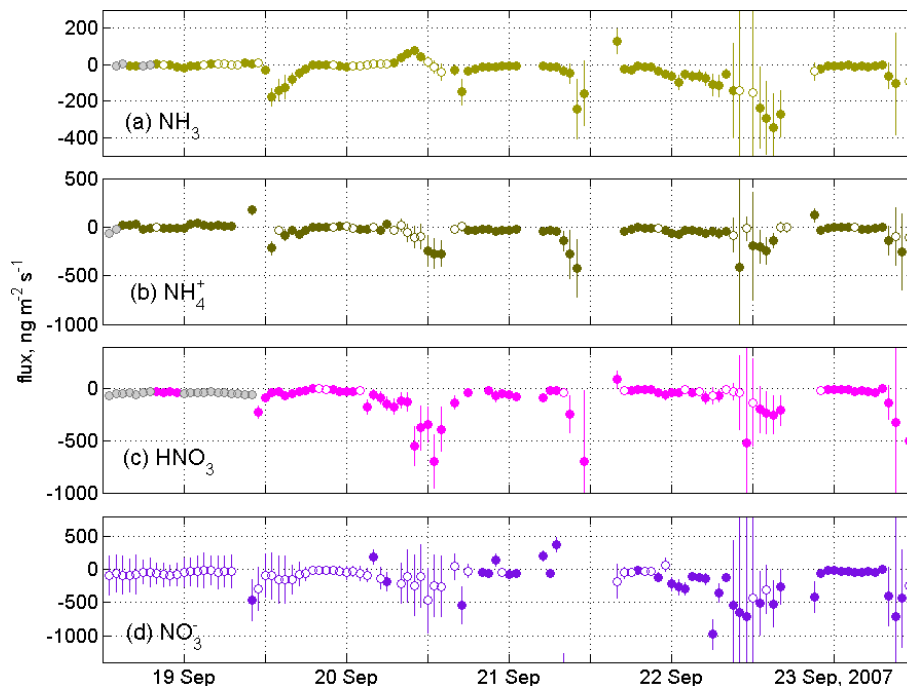


**Fig. 13.** Fluxes of **(a)**  $\text{NH}_3$ , **(b)** particulate  $\text{NH}_4^+$ , **(c)**  $\text{HNO}_3$ , and **(d)** particulate  $\text{NO}_3^-$  during EGER. Error bars are derived from both,  $\sigma_{v_r}$  and  $\sigma_{\Delta C}$ . Hollow symbols denote flux values that are derived from  $\Delta C$  that are insignificantly different from zero (Sect. 4.2). Grey circles denote flux values calculated with one or both concentrations below the LOD.

[Title Page](#)[Abstract](#)[Introduction](#)[Conclusions](#)[References](#)[Tables](#)[Figures](#)[◀](#)[▶](#)[◀](#)[▶](#)[Back](#)[Close](#)[Full Screen / Esc](#)[Printer-friendly Version](#)[Interactive Discussion](#)

**An analysis of  
precision  
requirements and  
flux errors**

V. Wolff et al.

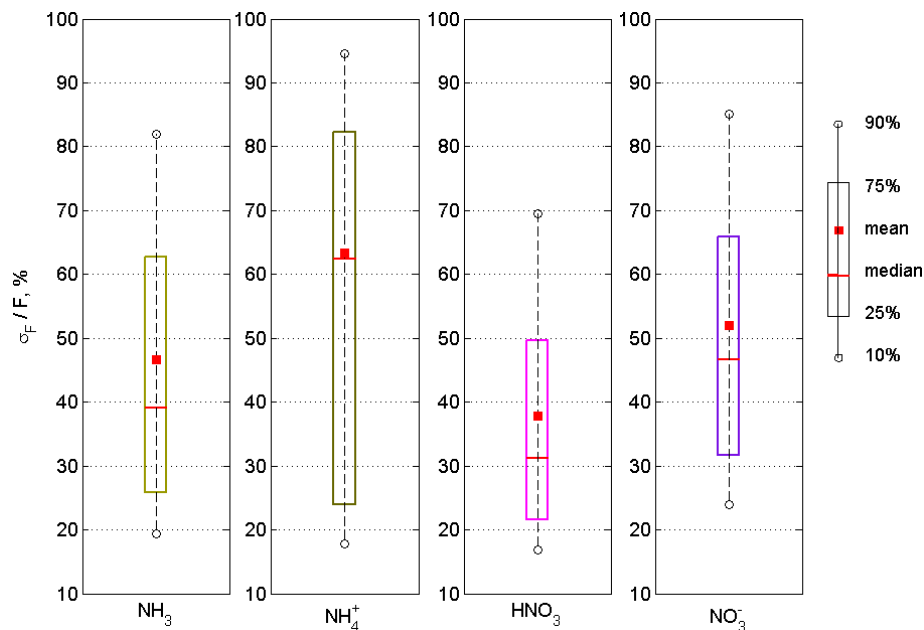


**Fig. 14.** Statistical representation of the relative flux error ( $\sigma_F/F$ ) for  $\text{NH}_3$ , particulate  $\text{NH}_4^+$ ,  $\text{HNO}_3$ , and particulate  $\text{NO}_3^-$  during NEU in Oensingen (Switzerland), 2006 (managed grassland ecosystem). Only data derived from significant values of  $\Delta C$  are used.

Title Page

Abstract

Introduction

Conclusions

References

Tables

Figures

◀

▶

◀

▶

Back

Close

Full Screen / Esc

Printer-friendly Version

Interactive Discussion

**An analysis of  
precision  
requirements and  
flux errors**

V. Wolff et al.

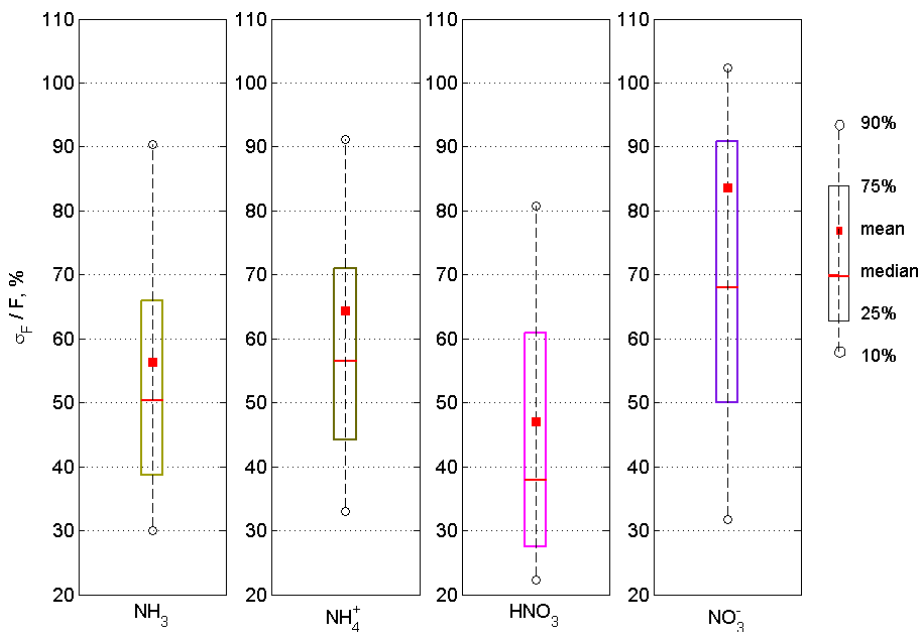


**Fig. 15.** Statistical representation of the relative flux error ( $\sigma_F/F$ ) for  $\text{NH}_3$ , particulate  $\text{NH}_4^+$ ,  $\text{HNO}_3$ , and particulate  $\text{NO}_3^-$  during EGER in Waldstein (Germany), 2007 (spruce forest ecosystem). Only data derived from significant values of  $\Delta C$  are used.

Title Page

Abstract

Introduction

Conclusions

References

Tables

Figures

◀

▶

◀

▶

Back

Close

Full Screen / Esc

Printer-friendly Version

Interactive Discussion